

RESEARCH

Open Access



HIV-1 escapes from N332-directed antibody neutralization in an elite neutralizer by envelope glycoprotein elongation and introduction of unusual disulfide bonds

Tom L. G. M. van den Kerkhof^{1,2}, Steven W. de Taeye¹, Brigitte D. Boeser-Nunnink², Dennis R. Burton^{3,4}, Neeltje A. Kootstra², Hanneke Schuitemaker^{2,5}, Rogier W. Sanders^{1,6*} and Marit J. van Gils^{6*}

Abstract

Background: Current HIV-1 immunogens are unable to induce antibodies that can neutralize a broad range of HIV-1 (broadly neutralizing antibodies; bNAbs). However, such antibodies are elicited in 10–30 % of HIV-1 infected individuals, and the co-evolution of the virus and the humoral immune responses in these individuals has attracted attention, because they can provide clues for vaccine design.

Results: Here we characterized the NAb responses and envelope glycoprotein evolution in an HIV-1 infected “elite neutralizer” of the Amsterdam Cohort Studies on HIV-1 infection and AIDS who developed an unusually potent bNAb response rapidly after infection. The NAb response was dependent on the N332-glycan and viral resistance against the N332-glycan dependent bNAb PGT135 developed over time but viral escape did not occur at or near this glycan. In contrast, the virus likely escaped by increasing V1 length, with up to 21 amino acids, accompanied by the introduction of 1–3 additional glycans, as well as 2–4 additional cysteine residues within V1.

Conclusions: In the individual studied here, HIV-1 escaped from N332-glycan directed NAb responses without changing the epitope itself, but by elongating a variable loop that shields this epitope.

Keywords: HIV-1, N332, Envelope glycoprotein, Glycans, Broadly neutralizing antibodies, Variable regions, Cysteines

Background

The development of a safe and protective HIV-1 vaccine is a major challenge. Although progress has been made over 30 years of research, there is no immunogen that can efficiently elicit protective humoral immunity. The HIV-1 envelope glycoprotein spike (Env) on the viral membrane is the sole target for neutralizing antibodies (NAbs), and therefore designing an Env-based immunogen capable of inducing antibodies that can neutralize diverse globally circulating viral variants (broadly neutralizing antibodies; bNAbs) is an obvious vaccine strategy to pursue.

In 10–30 % of the HIV-1 infected individuals bNAbs develop, indicating that there are no insurmountable barriers for the induction of bNAbs by Env in humans [1–8]. Several passive immunization studies in non-human primates using bNAbs isolated from HIV-1 infected individuals have shown protection against HIV/SHIV acquisition, even with low bNAb doses and after repeated viral challenges [9–13]. Furthermore, 1 % of the HIV-1 infected individuals, termed “elite neutralizers”, develop exceptionally broad NAb responses, and some of these individuals develop a broad NAb response relatively quickly, i.e. within the first year after infection [8, 14]. Elite neutralizers might therefore serve as examples for Env-based vaccine design.

In infected humans, bNAbs appear to develop through co-evolution of HIV-1 Env and NAbs, probably via

*Correspondence: r.w.sanders@amc.uva.nl; m.j.vangils@amc.uva.nl

⁶ Department of Microbiology and Immunology, Weill Medical College, Cornell University, New York, NY 10065, USA

Full list of author information is available at the end of the article

multiple pathways. In one scenario, iterative cycles of viral escape from (early) autologous NABs and renewed NAB affinity maturation lead to NAB breadth [15–20]. This scenario is consistent with the large number of somatic mutations observed in HIV-1 bNABs [21–24]. In a second scenario, escape from one NAB specificity can result in the exposure or creation of a bNAB epitope elsewhere on the Env surface, resulting in an independent bNAB lineage [25, 26]. Viral factors that have been associated with bNAB development include high viral load and antigenic diversity, prolonged antigenic stimulation and polyreactivity [1, 2, 27–30], but also specific Env characteristics on early viruses, such as short variable loops and lower glycan content [31–35].

Despite this knowledge, inducing bNAB responses by means of vaccination has proven a major challenge. In fact, even inducing consistent NABs against the autologous, sequence-matched virus, with a vaccine based on a neutralization-resistant (Tier-2) primary isolate, has only been very recently achieved by immunizing with stabilized native-like trimers [36, 37]. The importance of viral evolution during Ab maturation, and in shaping bNAB responses, has led to the idea that sequential Env-based immunogens are required to steer Ab lineages towards becoming bNABs. Indeed, immunogenicity studies have shown improved NAB responses when using sequentially isolated Envs from an SHIV_{SF162p4} infected macaque or from HIV-1 infected individuals who developed breadth, although NABs were elicited only against neutralization-sensitive (Tier-1) viruses [38–40]. Therefore, studying Env evolution in infected individuals who eventually developed bNABs, in particular elite neutralizers, can provide information that benefits sequential Env-based immunogen strategies.

The native, pre-fusion Env spike is a heterotrimeric complex of three gp120 subunits non-covalently linked to three gp41 subunits that are derived from a gp160 precursor protein through proteolytic cleavage [41]. Gp120 is composed of five conserved regions (C1–C5), interspersed with five exposed variable regions (V1–V5). C1–C5 form the gp120 core that is crucial for binding to target cells and transmitting receptor-induced conformational changes to the fusion machinery in gp41. V1–V5, in particular V1, V2 and V4, are highly diverse as a consequence of mutations, recombinations, deletions, and/or insertions. V1–V3 are important trimer association domains interacting at the apex of the trimer [42–46]. The high variability in these domains is driven by the need to continuously escape from NABs and is facilitated by the high replication rate of the virus combined with the error prone reverse transcription process.

The *N*-linked glycans that are attached to 20–35 potential *N*-linked glycosylation sites (PNGS) on the backbone

of gp120 account for 50 % of the mass of the external Env domains [47], and are usually not seen as foreign by the immune system. Therefore glycans and highly variable regions provide a formidable viral defense to protect the conserved Env regions from NAB attack [48–52]. Yet by necessity bNAB epitopes frequently incorporate glycan components, indicating that they are not completely immunosilent.

To fold and maintain its intricate structure gp120 typically has 18 cysteine residues that form 9 disulfide bonds, and one additional disulfide bond is present in gp41 [53, 54]. Disulfide bonds are key structural elements for protein folding and function, which also explains why disulfide bonds are usually conserved within protein families [54]. The positions of the disulfide bonds in gp120 are highly conserved across all isolates of HIV and SIV (Los Alamos database). Additional cysteine residues in the variable regions have been observed in HIV-1 (Table 1), but more so in HIV-2 and SIV (in particular in V2) [55–59].

Here we have studied Env evolution in response to NAB pressure over time in an individual from the Amsterdam Cohort Studies on HIV-1 infection and AIDS (ACS) infected by intravenous drug use (IDU), who developed an elite bNAB response within 30 months post-seroconversion (post-SC) [14]. NAB responses developed against autologous and heterologous viruses and were strongly dependent on the glycan at position 332. Viral escape from these responses did not occur at or near the N332-glycan, but rather involved the elongation of V1, by up to 21 additional amino acids. This V1 extension coincided with the introduction of 2–4 additional cysteine residues and 1–3 glycans, and was accompanied by a fitness loss. These findings provide insights into how HIV-1 can escape from N332-directed bNAB responses without changing the epitope itself.

Results

Development of autologous NAB responses in elite neutralizer D16916

Individual D16916 entered the Amsterdam Cohort Studies (ACS) HIV-1 negative and seroconverted during active follow-up after infection with a clade B virus. In the first five years post-SC, this individual had stable CD4⁺ T cell numbers (average 395 cells/ μ l) and low to undetectable viral loads (Additional file 1: Fig. S1). We previously described the development of the bNAB responses in this individual [14]. At 38 months, D16916 qualified as an elite neutralizer, neutralizing all viruses of a six-virus panel that is representative of global HIV-1 variation, at a geometric mean midpoint titer of 978 (Fig. 1a). By this standard this individual has the broadest and most potent neutralization observed in the ACS. Furthermore,

Table 1 Relative occurrence of non-conserved cysteine residues in V1, V2 and V4 in HIV-1 subtypes

HIV-1 subtype	n ^a	V1 region			V2 region				V4 region			
		Canonical ^b	Plus 2 cysteines	Plus 4 cysteines	Normal	2 cysteines	4 cysteines	Total	Canonical	Plus 2 cysteines	Plus 4 cysteines	Total
A	208	98.6	1.4	0	99.5	0.5	0	100	100	0	0	100
B	1338	94.4	5.5	0.1	99.9	0.1	0.1	100	99.9	0.1	0	100
C	952	94.5	5.1	0.3	99.7	0.3	0	100	99.5	0.5	0	100
D	101	99	1.0	0	100	0	0	100	100	0	0	100
F	39	100	0.0	0	100	0	0	100	100	0	0	100
G	61	73.8	26.2	0	100	0	0	100	100	0	0	100
Other	960	96.9	3.1	0	99.6	0.4	0	100	89.5	10.5	0	100
Total	3659	95.2	4.7	0.1	99.7	0.2	0	100	97.1	2.9	0	100

^a The number of Env sequences used to calculate the percentage of viruses with canonical or non-conserved cysteine residues per subtype

^b The percentage of viruses with normal or non-conserved cysteine residue

a Heterologous neutralization

Time post-SC (months)	94UG103 (A)	92BR020 (B)	JRCSF (B)	93IN905 (C)	MGRM-C-026 (C)	92TH021 (CRF01_A E)	aMLV	Geometric mean midpoint titer
8	<40	215	48	<40	74	<40	<40	43
11	85	1012	115	<40	154	<40	<40	92
14	150	1670	179	88	317	<40	<40	171
19	116	1310	181	159	262	<40	<40	169
22	175	1832	205	369	427	<40	<40	243
26	375	2030	480	338	534	<40	<40	331
30	505	2870	795	635	1354	<40	<40	520
34	712	3798	1218	1245	1970	<40	<40	738
38	1121	2271	1039	1509	4234	52	<40	978

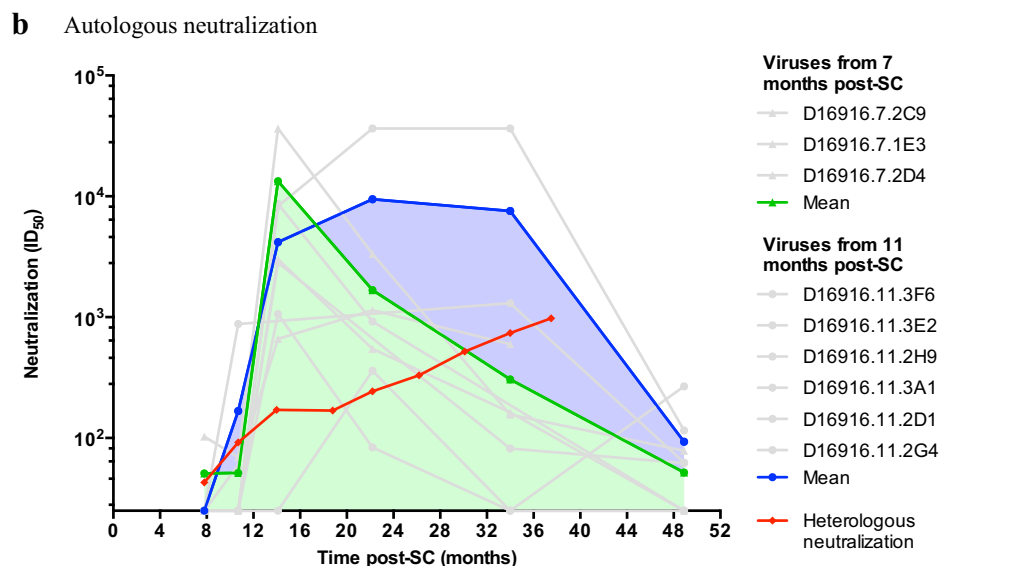


Fig. 1 Development of heterologous and autologous NAB responses in elite neutralizer D16916. **a** Neutralizing activity over the course of HIV-1 infection against the individual viruses of a 6-virus panel that is representative for HIV-1 variation worldwide [8, 32]. The ID₅₀ against each virus as well as the geometric mean midpoint titer for all 6 viruses combined are given for D16916 sera taken 8, 11, 14, 19, 22, 26, 30, 34 and 38 months post-SC. A color scale is used to indicate low (green) to high (red) ID₅₀ values. **b** Longitudinal neutralization of autologous viruses. The mean ID₅₀ values of longitudinal sera (x-axis) against the autologous viruses (3 for month 7 and 6 for month 11, all in grey) are plotted in green (month 7) and blue (month 11). The red line indicates the geometric mean midpoint titer against the heterologous 6-virus panel from **a** [14]

neutralization of multiple heterologous Tier-2 viruses was observed at around 8 months, and broad neutralization, defined as a geometric mean midpoint titer of >100, was observed around 11 months, which is unusually early [14].

To gain more insight into the unusually rapid heterologous NAb response, we first studied the development of the autologous NAb response at and preceding the 11 month time point (Fig. 1b). Therefore, we tested three and six viral isolates from 7 and 11 months post-SC, respectively. We observed low neutralizing activity

in serum from 8 months against one out of three viruses from 7 months, and no activity against any of the other viruses from 7 and 11 months tested. Serum neutralization against the month 7 viruses rapidly increased until it peaked at 14 months, after which it declined very rapidly. The increase in neutralizing activity could also be observed against viruses from 11 months, although the activity against these viruses remained rather stable between 14 and 34 months before declining. Thus, around a year post-SC, i.e. when heterologous NAb responses first appeared, this individual had developed

Table 2 N332-directed heterologous NAb responses in elite neutralizer D16916

	ID ₅₀ ^a		Fold ^d reduction
	WT ^b	N332A	
92BR020	1711	49	35
JRCSE	211	60	3.5
MGRM-C-026	269	70	3.9
	T332N ^c	WT (T332)	
BG505	63	<40	>1.5

^a 50 % inhibitory dilution (ID₅₀)

^b ID₅₀ of month 14 serum tested against the 92BR020 and JRCSE (both clade B) and MGRM-C-026 (clade C) viruses and their N332A mutants

^c ID₅₀ of month 30 serum tested against the BG505 virus (clade A) and its T332N mutant

^d The fold-reduction in neutralization as a consequence of the lack of the N332-glycan

strong autologous NAb responses against the viruses that were present at 7 months post-SC. Whether earlier autologous NAb responses against the preceding viruses were present, could not be tested because such samples were not available for analysis.

N332-directed bNAb responses in elite neutralizer D16916

Five viruses of the six-virus panel were neutralized by serum from individual D16916 as early as 14 months after infection. The 92TH021 virus was an exception and was only very weakly neutralized by month 38 (Fig. 1a). We noted that the five sensitive viruses had the PNGS at position 332, which is frequently targeted by bNAb responses [60], whereas 92TH021 contains the PNGS at position 334. To assess whether the bNAb response in individual D16916 was N332-glycan dependent, we measured the neutralization activity of serum from 14 months against three viruses of the six-virus panel in comparison with their N332A glycan knock-out variants: JRCSE, 92BR020 (both clade B viruses) and MGRM-C-026 (a clade C virus) [61]. Unfortunately, changing the glycan from position 334–332 in 92TH021 did not yield an infectious virus. We observed a marked decrease in neutralization sensitivity for the three N332A variants, when compared with the wild-type (WT) viruses (Table 2). We also tested serum from 30 months, when elite bNAb activity was present, against the Tier-2 subtype A BG505 virus, which naturally lacks the N332-glycan, as well as the BG505 T332N glycan knock-in mutant [62]. While the WT BG505 virus was not neutralized (10 % neutralization at a 1:40 dilution), we did observe neutralization of the T332N glycan knock-in virus (77 % neutralization at a 1:40 dilution; see also Table 2). These

data suggest that a substantial proportion of the bNAb response in elite neutralizer D16916 is directed against the N332-glycan.

Development of viral resistance to N332-directed bNAb PGT135, as well as bNAbs b12 and 12A21

To study the effect of the N332-directed NAb response on the viral evolution in individual D16916 we tested longitudinally isolated viruses for their sensitivity to N332-directed bNAbs PGT121, PGT126, PGT128, PGT135 and 2G12. No differences were observed in the neutralization sensitivity of viruses from month 7 and 11 to the N332-directed bNAbs, except for PGT135 (Fig. 2a; Additional file 2: Fig. S2A–D). While, 9 out of 10 viruses isolated from month 7 were sensitive to PGT135, only 1 out of 9 viruses from month 11 was sensitive to PGT135. Thus, from month 7 to month 11, the majority of viruses acquired resistance to the N332-directed bNAb PGT135 (>14-fold when comparing the median 50 % inhibitory concentration (IC₅₀) values, $p = 0.0016$). In addition, we also tested bNAbs targeting other epitopes. We observed, to a lesser extent, development of resistance against the CD4bs-directed bNAbs b12 and 12A21 (2.5-fold, $p = 0.0072$ and 3-fold, $p = 0.01$, respectively; Fig. 2b, c). In contrast, we observed an increased sensitivity to bNAbs PG16 and PGT145, directed against a quaternary glycan-dependent V2 epitope (by >7-fold, $p = 0.0027$ and >36-fold, $p = 0.0007$, respectively; Fig. 2d, e). We did not find significant differences in the neutralization sensitivity to bNAbs VRC01, PG9, and 8ANC195 (Additional file 2: Fig. S2E–G).

Lack of viral escape mutations in the N332-directed bNAb epitope

Since we observed the development of viral resistance to PGT135, b12 and 12A21, we studied the evolution of the epitopes of these bNAbs. We sequenced the complete gp160 *env* from multiple viruses from different time points (Fig. 3a). Phylogenetic analyses showed that, with one exception, the month 7 and month 11 sequences formed separate clusters (Additional file 3: Fig. S3). Interestingly, we did not observe escape mutations at the N332-glycan, nor did we find escape mutations anywhere else in the PGT135 epitope (Additional file 4: Fig. S4A), suggesting that changes outside the PGT135 epitope were responsible for the increase in PGT135-resistance from month 7 to 11.

We did observe mutations in the b12 and 12A21 epitopes at month 11 compared to month 7, notably at position 475, a contact residue for b12, and at position 462, a contact residue for 12A21 (Additional file 4: Fig. S4B). However, none of these changes were

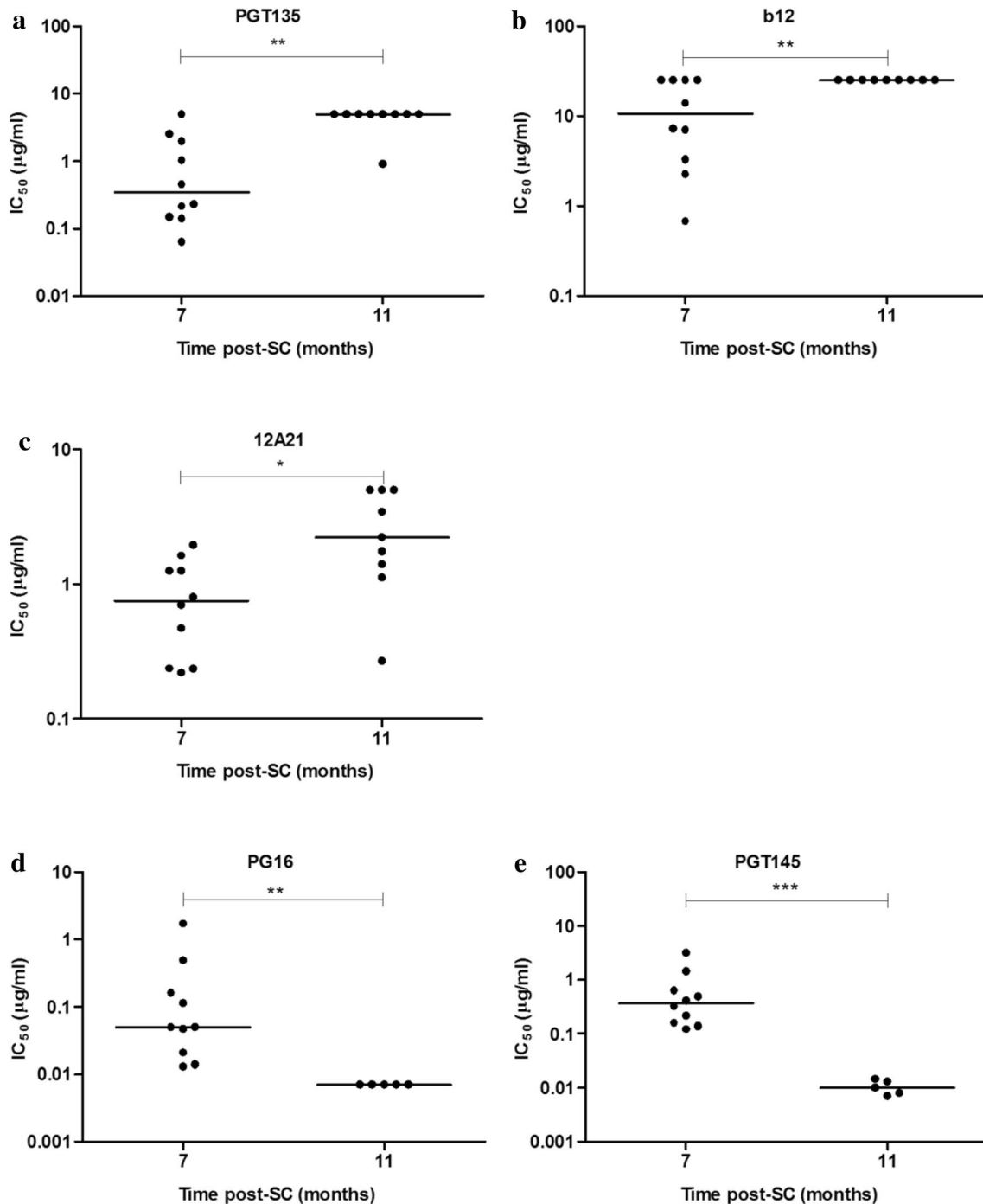
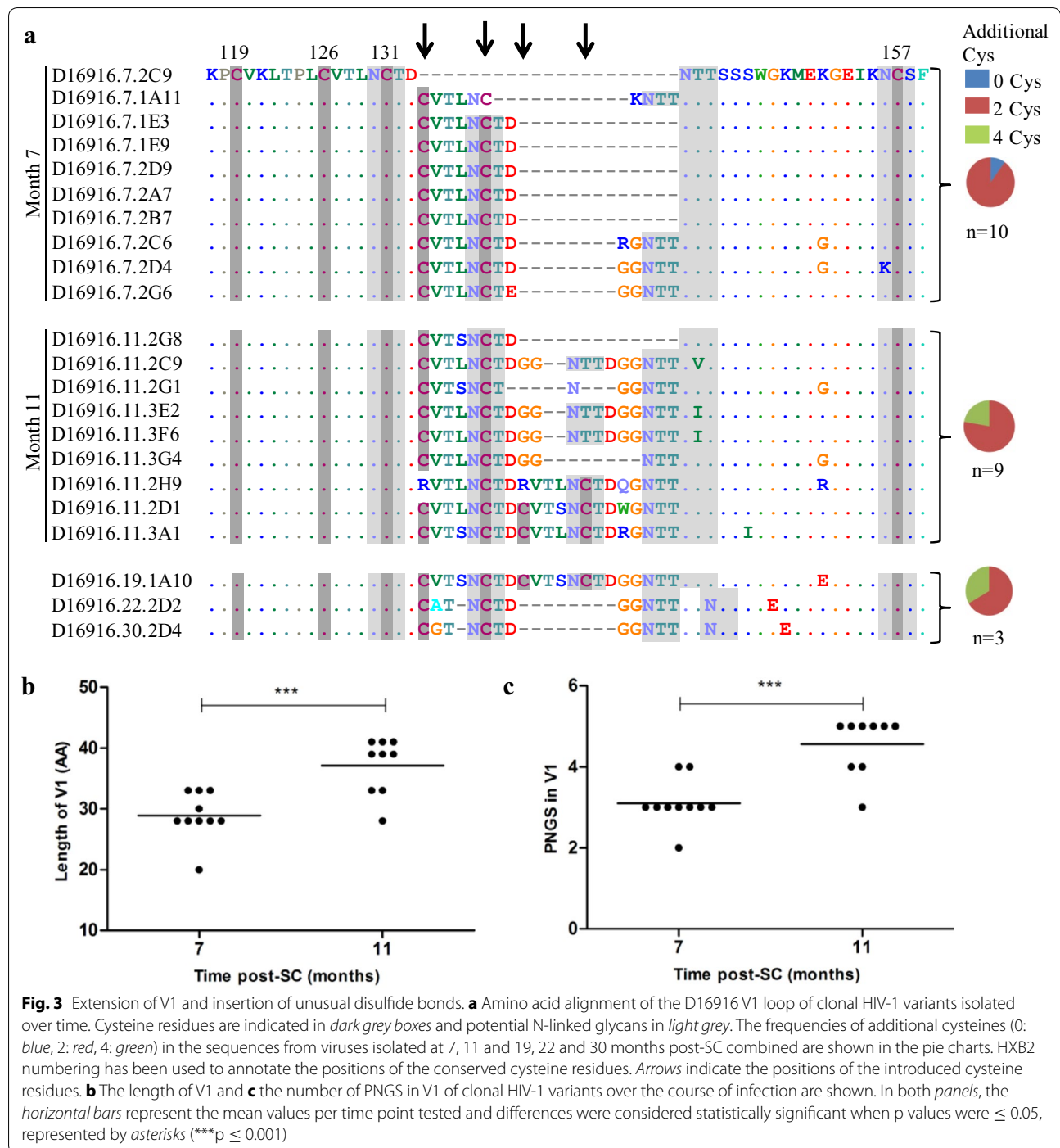


Fig. 2 Sensitivity of viral isolates from individual D16916 to bNAbs. Clonal HIV-1 variants from 7 and 11 months post-SC were tested for their neutralization sensitivity against bNAbs PGT135 (a), b12 (b), 12A21 (c), PG16 (d) and PGT145 (e) and grouped according to their target epitope OD-glycan, CD4-bs and V1V2 apex. The graphs show IC₅₀ values for each virus isolate, as determined by linear regression. Differences were considered statistically significant when p values were ≤ 0.05, represented by asterisks (*p ≤ 0.05; **p ≤ 0.005, ***p ≤ 0.001). The horizontal bars represent the median IC₅₀ value per time point

associated with increased resistance to b12 or 12A21, when sensitivity of specific viral clones and their sequences were compared. The increase in neutralization

sensitivity for PG16 that developed from month 7 to 11 could also not be explained by mutations in the known epitope, as there were none (Additional file 4: Fig. S4C).



Elongation of V1 with insertions of unusual disulfide bonds
 Since we did not find mutations in the bNAb epitopes that could explain the increase in neutralization resistance we studied the evolution of the entire gp160 sequence. We identified many amino acids that changed from month 7 to month 11 and these amino acids were scattered across the gp160 sequence. Some of these

changes became fixed in the viral population, but none of them stood out as likely candidates to explain the altered neutralization profile.
 However, we observed a significant increase in the length of gp160 and the number of PNGS from month 7 to month 11 (mean of 827 vs. 836 amino acids, $p = 0.0009$, mean of 30 vs. 32 PNGS, $p < 0.0001$,

respectively). Both were mostly attributable to an increase in V1 length (mean of 29 vs. 37 amino acids, $p = 0.0006$, mean of 3 vs. 4.5 PNGS, $p = 0.0001$, respectively; Fig. 3b, c). The additional PNGS in the V1 were all NXT motifs, which have a higher probability to become glycosylated compared to NXS motifs [63–65].

At 7 months, we found one virus with a short V1 (20 amino acids) while the other 9 sequences showed V1 elongation by 8, 10, or 13 additional amino acids, including one or two extra PNGS (Fig. 3a). The elongation of the V1 was likely caused by an 8 amino acid duplication of the sequence CVTLNCTD containing 2 extra cysteines and one PNGS (5 isolates), followed by the insertion of an additional 5 amino acids (GGNTT or RGNTT), including an additional PNGS (3 isolates). The additional 2 cysteines are likely to pair and form a disulfide bond in an “oven mitt” structure (Additional file 5: Fig. S5B) [59].

At 11 months we observed three isolates with similar features as described for the isolates from 7 months containing 2 additional cysteines. Remarkably, in three other isolates the V1 length was further increased (to 39 amino acids), with a 6 amino acid duplication of the sequence DGGNTT. Interestingly, in three other virus isolates the 8 amino acid sequence CVTNLCTD was again duplicated and further mutated, resulting in a V1 with 4 extra cysteines (2 isolates), while in the last virus isolate the first cysteine of each 8 amino acid repeat was replaced by an arginine, restoring the number of cysteines to +2 (Additional file 5: Fig. S5C). The 4 extra cysteines might form 2 extra cysteine bridges, with “oven mitt” structures, but an alternative structure is now also possible (Additional file 5: Fig. S5D–F). The longest V1 sequences (clones 2H9, 2D1 and 3A1 at month 11 and clone 1A10 at month 19) have a V1 of 41 amino acids, i.e. 21 amino acids longer than the shortest V1 (clone 2C9 at month 7). For comparison, the average V1 length in Env sequences in the Los Alamos Database is 27 amino acids, with 95 % of the sequences falling in the range of 15–39 amino acids, illustrating that a V1 of 41 amino acids is unusually long.

We could only isolate one virus from 19, 22 and 30 months (Fig. 3a). The virus isolated at 19 months had a V1 sequence that was very similar to the unusually long month 11 V1 containing 4 extra cysteines, while the month 22 and 30 sequences contained moderately long V1 sequences with two extra cysteine residues (Fig. 3a).

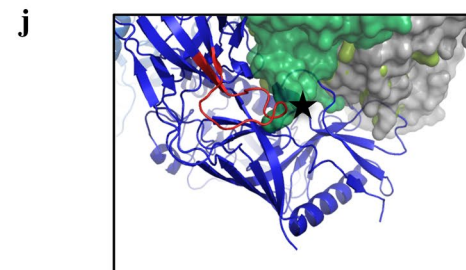
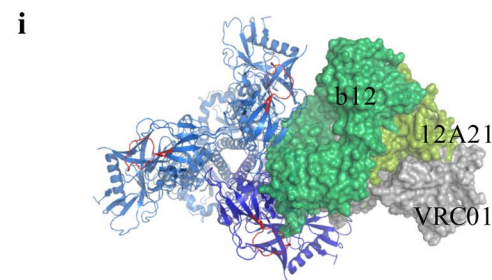
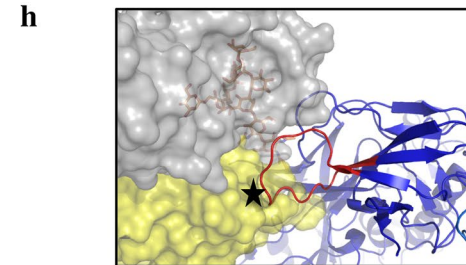
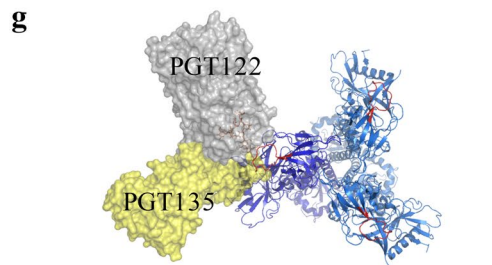
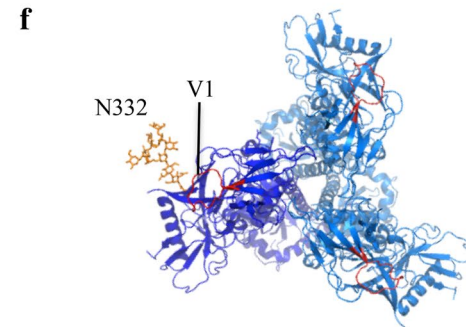
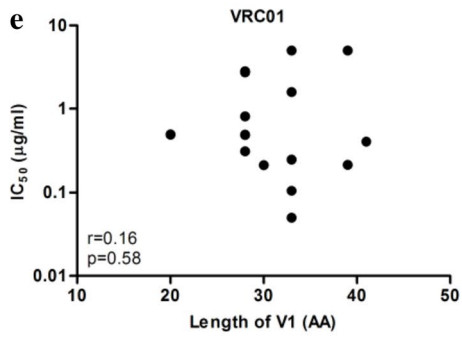
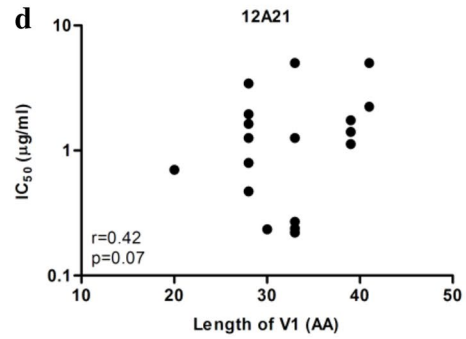
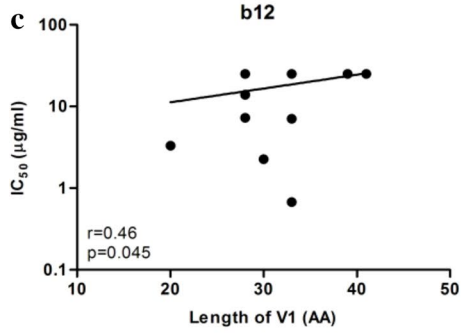
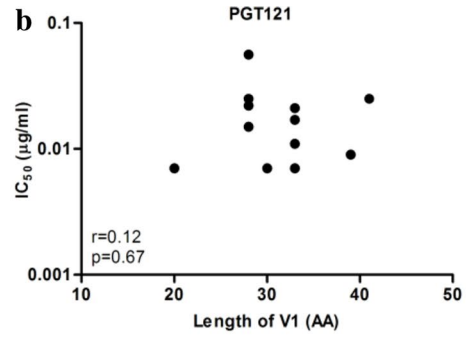
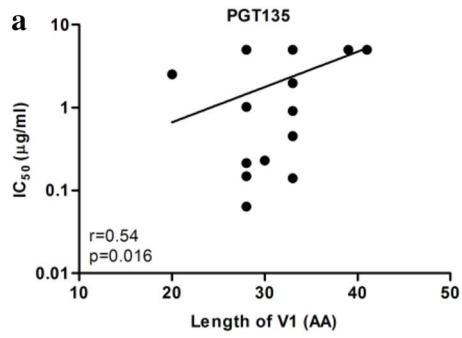
We analyzed the frequency of additional cysteines in V1, as well as V2 and V4 in natural HIV and SIV isolates. The presence of additional cysteines in V1 is common in HIV-2 and SIV (Los Alamos Database), but rare in HIV-1 (Table 1). 4.7 % of HIV-1 isolates contain two extra cysteines in V1, while 4 extra cysteines are present in only 0.1 % of HIV-1 sequences, illustrating that the Env protein in individual D16916, who developed elite NAB responses, evolved to have rather unusual properties.

Involvement of V1 length in resistance to bNAbs PGT135, b12 and 12A21

The elongation of the V1 from month 7 to 11, and the accompanying introduction of additional cysteine residues, led us to speculate that the V1 was responsible for the increased resistance against bNAbs PGT135, b12 and 12A21. For PGT135, we observed a statistically significant positive correlation between V1 length and neutralization resistance ($r = 0.54$, $p = 0.016$; Fig. 4a). Inspection of the Env structure in complex with PGT135 reveals that a longer V1 region could indeed clash with PGT135 (Fig. 4g, h). For PGT121, which also targets the N332-glycan, we did not observe a correlation between the length of the V1 region and neutralization sensitivity (Fig. 4b), which might be related to the different angle of approach of the bNAb, thereby avoiding a clash with V1 (Fig. 4h). In addition, we observed a significant positive correlation between V1 length and neutralization resistance for b12 and a trend for 12A21, both directed against the CD4bs ($r = 0.46$, $p = 0.045$ and $r = 0.42$, $p = 0.07$, respectively; Fig. 4c, d). These bNAbs can also clash with unusually long V1 regions (Fig. 4i, j), while VRC01, another CD4bs bNAb for which no correlation between the length of V1

(See figure on next page.)

Fig. 4 Involvement of V1 length in resistance to bNAbs PGT135, b12 and 12A21. Correlation plots between the V1 length and neutralization sensitivity for mAbs PGT135 (a), PGT121 (b), b12 (c), 12A21 (d), and VRC01 (e). The r and p values for the linear regression are given. For correlations that were statistically significant, the regression line is shown. (f) Top view of the Env trimer with one protomer shown in *dark blue* and the other protomers in *light blue*. The V1 loops are indicated in *red* and the N332-glycan is shown on one protomer. (g) View of the trimer in the same orientations as in f in complex with PGT135 (*yellow*) and PGT122 (*gray*). We used PGT122 in our figure instead of PGT121 since the HIV-1 Env trimer structures were solved in complex with PGT122, whereas for PGT121 the structure was only solved in complex with a glycan [42] or recently a complex of a PGT121 precursor in complex with the HIV-1 Env trimer [120]. It was shown that PGT121 and PGT122 bind to the Env protein with the same angle of approach in a very similar way. (h) Detailed view of the expected clash of PGT135 with the V1 loop indicated by an *asterisk*. (i) View of the trimer in the same orientations as in f in complex with b12 (*green*) and 12A21 (*dark green*) and VRC01 (*gray*). (j) Detailed view of the expected clash of b12 with the V1 loop indicated by an *asterisk*. The figures were drawn using pymol (www.pymol.org) by aligning the gp120 structures of 4JM2.pdb (gp120 plus PGT135; PMC3823233 [60]), 2NY7.pdb (gp120 plus b12; PMC2584968 [121]), 4JPW.pdb (gp120 plus 12A21; PMC3792590 [122]), and 3NGB.pdb (gp120 plus VRC01; PMC2981354 [123]) with the *dark blue* protomer of the BG505 SOSIP664 trimer in complex with PGT122 and 35O22 (4TVP.pdb [43])



(See figure on next page.)

Fig. 5 Accommodation of long V1, associated with viral fitness loss, by compensatory mutations. **a** Viral replication of clonal viral isolates from month 7 versus month 11 with the horizontal bars representing the median p24 values over the viruses isolated at that time point. **b** Linear regression between viral replication, expressed as p24 production per day, and V1 length for viruses from month 7 and 11. Virus isolates are colored based on number of additional cysteine residues in their V1 (0: blue, 2: red, 4: green). **c** V1 sequence alignment of representative virus isolates from individual D16916 with 0, 2 and 4 additional cysteines (clones D16916.7.2C9, D16916.7.1E3, D16916.11.2D1), as well as HIV-1_{LAI}, HIV-1_{LAI} mutants 1 and 2, and their revertants. **d** CA-p24 ELISA of HIV-1_{LAI} and mutant virus stocks, produced by transient transfection of HEK293T cells. **e** TZM-bl cells were infected with 500 pg CA-p24, and infectivity was measured after 48 h infection. **f** Schematic V1/V2 topology. β -strands are depicted as purple arrows and disulphide bonds as yellow lines. The V1 and V2 loop are indicated in green and blue lines, respectively. The substitutions designed to restore the epitopes for bNAbs PG9 and PG16 are underlined and the locations of the HIV-1_{LAI} reversions are indicated in bold. **g** Ribbon diagram of **f** with the position of the HIV-1_{LAI} reversions indicated as red spheres (except L \rightarrow P at the fourth position of the insert) and labeled according to their position in the linear sequence. Note that the elongated V1 with additional cysteine residues is not depicted

and neutralization sensitivity was found (Fig. 4e), targets the CD4bs with an angle that avoids the V1 (Fig. 4i, j).

Association of V1 length with loss of viral fitness

Based on the low occurrence of long V1 sequences with extra disulfide bonds in natural isolates, we hypothesized that the elongation of the V1 and the inclusion of extra cysteine residues, possibly a consequence of NAb pressure, might have a negative impact on viral fitness. We analyzed the replication kinetics of all virus isolates from 7 and 11 months on phytohemagglutinin (PHA) stimulated peripheral blood mononuclear cells (PBMCs). We observed that there was a significant difference between the replication rates of the viral isolates from 7 and 11 months ($p = 0.0041$, Fig. 5a), and a significant negative correlation between the replication kinetics and the V1 length ($r = -0.62$, $p = 0.0044$; Fig. 5b). Thus, viruses isolated later during infection harboring longer V1 had lower replication rates compared to earlier viruses harboring a shorter V1. These data support the hypothesis that the virus present in individual D16916 was under selection pressure from NAbs to generate and preserve gp160 proteins with unusually long V1 loops containing additional cysteines that were accompanied with a decrease in gp160 function.

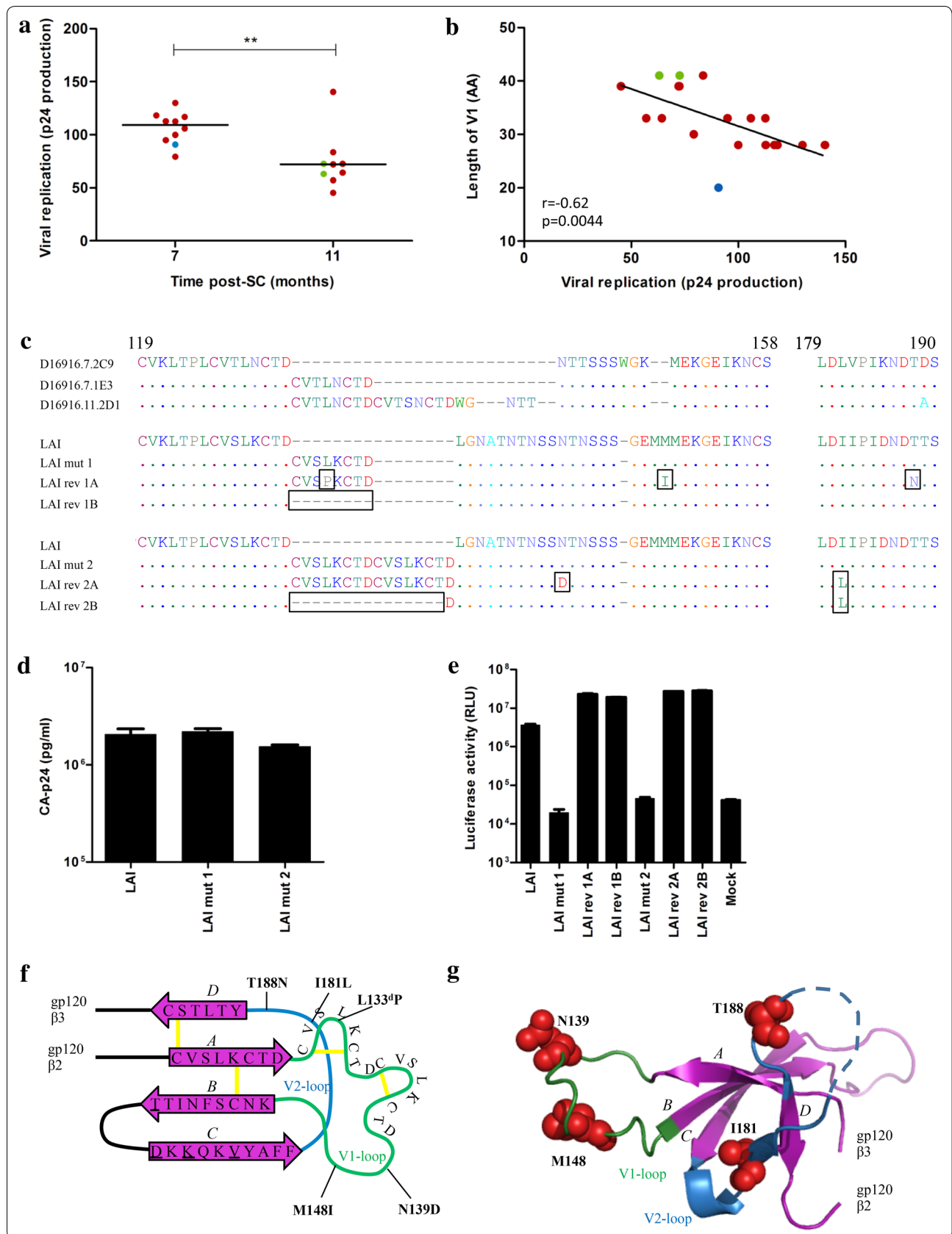
Accommodation of elongated V1 loops with additional cysteine bonds in a different virus isolate

To answer the question whether the long V1 sequences with additional cysteine residues were isolate-specific or could be incorporated into an unrelated HIV-1 strain, we investigated the infectivity of variants of the HIV-1_{LAI} isolate (containing 4 substitutions to facilitate PG9/PG16 binding: S162T, G167D, V169K and E172V) in which the V1 sequences were extended with 8 or 16 amino acids, based on the increase in V1 length observed in individual D16916. In mutant 1, the V1 was extended by 8 amino acids (CVSLKCTD; based on month 7 isolate D16916.7.1E3) and in mutant 2 by 16 amino acids (CVSLKCTDCVSLKCTD; based on month 11 isolate D16916.11.2D1), harboring 2 or 4 extra cysteines,

respectively (Fig. 5c). Virus stocks were generated in HEK293T cells and the two mutant viruses were analyzed for their ability to infect TZM-bl cells. We observed that mutant 1 and 2 produced similar amounts of capsid (CA)-p24 antigen compared to wild-type virus (Fig. 5d), but were not able to infect TZM-bl cells (Fig. 5e). These data suggest that the long V1 sequences cannot be introduced in any virus isolate and/or that compensatory changes are required to do so.

Next we performed in vitro virus evolution experiments using the HIV-1_{LAI} mutant. Four independent cultures of SupT1 cells were transfected with the molecular clones of either HIV-1_{LAI} mutant 1 (cultures 1A and 1B) or mutant 2 (cultures 2A and 2B). The transfected cells were maintained for 3 months, and the cultures were inspected every week by eye for the presence of syncytia and by CA-p24 enzyme linked immunosorbent assay (ELISA). For mutant 1, replicating virus was identified 2 and 3 weeks post-transfection (cultures 1B and 1A, respectively), whereas for mutant 2 replication was observed after 5 weeks (both cultures). In contrast to the original mutant viruses, the evolved viruses obtained after 3 months of culturing were able to infect TZM-bl cells (Fig. 5e). Both HIV-1_{LAI} and the evolved viruses were resistant to all N332-dependent bNAbs as well as the apex bNAbs, precluding analyses to study the differences in sensitivity to N332-directed specificities in the context of the HIV-1_{LAI} isolate (data not shown).

Total cellular DNA was extracted from the infected cells at 3 months post-transfection. The *env* sequences revealed mutations in all four cultures (indicated by boxes; Fig. 5c). In culture 1A the 8 amino acid insertion was maintained, but a substitution was observed at the fourth residue of the inserted sequence (L133^dP), as were substitutions further downstream in V1 and V2 (M148I and T188N). In the 1B culture we observed the deletion of the introduced 8 amino acids. In culture 2A we found two substitutions: N139D in V1 and I181L in V2, whereas in culture 2B we observed the deletion of all 16 introduced amino acids except for one aspartic acid, as well as an I181L substitution.



Interestingly, we found that the I181L substitution was present in all the viral isolates from individual D16916, suggesting that the presence of a leucine at position 181 might facilitate the V1 insertion. Furthermore, the T188N substitution that emerged during evolution in culture 1B was also observed in one viral isolate (data not shown). The 181 and 188 residues are located at the base of V2 that interacts with the base of V1 and they might therefore contribute to the appropriate positioning of the elongated V1 (Fig. 5f, g).

Discussion

To guide Env-based vaccine design, it is important to understand the mechanisms that are involved in the development of bNAb responses and viral escape from them. Here we studied virus evolution in individual D16916 of the ACS with unusually potent and broad NAb responses, which developed much faster than usually seen, i.e. within 1 year as opposed to 2–3 years [14], making individual D16916 a particularly attractive case to inform vaccine design.

In concordance with other studies, we observed that the autologous NAb responses in individual D16916 developed in parallel with the heterologous NAb response development [2, 17, 18, 20, 26, 51, 66, 67], supporting the view that iterative cycles of NAb escape and renewed affinity maturation lead to increased neutralization breadth [16–20]. When dissecting the heterologous NAb response we observed that this response was dependent on the glycan at position 332 of Env. This glycan is a central feature of the supersite of immune vulnerability on the glycosylated outer domain of gp120 that is targeted by multiple bNAbs [60], and is commonly targeted by NAb responses in HIV-1 infected individuals [68]. Moore et al. showed that in two individuals the appearance of the N332-glycan on Env, which allowed immune escape early during infection, created a new epitope on the autologous virus that triggered the development of N332-directed bNAbs [25]. We were not able to generate viruses from before 7 months post-SC, and therefore we cannot determine whether a similar pathway was followed in individual D16916.

Various known N332-directed bNAbs have been isolated from different HIV-1 infected individuals and are derived from different germline lineages. Extensive studies showed that most of these bNAbs interact differently with the N332-glycan, even when the bNAbs are of the same antibody lineage (such as PGT121, PGT122 and PGT124), probably due to different maturation pathways [69, 70]. In addition to the targeting of the N332-glycan, these bNAbs often also recognize other glycans, such as N137, N156, N301, as well as protein backbone. In individual D16916 we observed viral escape from

N332-directed bNAb PGT135 [60] but not from other N332-glycan targeting bNAbs, suggesting that PGT135-like N332-directed bNAbs were elicited by this individual.

Escape from N332-directed (b) NAbs has been reported, both in HIV-1 infected individuals and in infected macaques and humanized mice that received N332-directed bNAbs as immunotherapy. Such escape is usually mediated via a direct mutation of the N332-glycan or mutations elsewhere in the target epitope [25, 71–75]. In contrast, in individual D16916 it appears that viral escape from N332-directed bNAbs was mediated by a large increase in V1 length, rather than direct mutation of the N332-glycan or residues nearby. Escape via elongation of V1, in combination with mutations in other variable regions, but not the removal of the N332-glycan, was also observed in one rhesus macaque that was inoculated with SHIV_{AD8-LN} and developed potent bNAbs targeting the N332-glycan [76, 77]. However, the elongated V1 (by 6 amino acids) was not the principal determinant of viral resistance in this animal, as it was shown that mutations in V3 were responsible for the escape [72]. The viral escape in individual D16916 from N332-directed, PGT135-like NAb responses through V1 masking is supported by the positive correlation between the V1 length and the increased resistance to PGT135. Multiple studies have described that an increase in variable loop length is a shielding mechanism to protect other bNAb epitopes from antibody recognition [33, 51, 78–88]. The viral escape from N332-directed bNAbs, and to a lesser extent resistance to CD4bs bNAbs, via an elongated and stabilized V1, could be achieved by intraprotomer or interprotomer masking of the N332 and/or CD4bs, and both scenarios are compatible with the trimer structure (Fig. 4) [43, 89–92].

Remarkably, we observed that the elongation of the V1 was accompanied by the introduction of additional cysteine residues, which is a rare phenomenon. As some studies suggest that viral escape from autologous NAbs can result in reduced viral replication, whereas others observed minimal fitness cost [31, 67, 93–97], we were interested if an elongated V1 with additional cysteine residues could indeed reduce viral replication. We did not find a significant difference in replication rate or neutralization sensitivity for bNAbs when comparing viruses that harbored 0, 2 or 4 extra cysteines in the V1 (data not shown), however longer V1 loops did correlate with reduced replication rates. Rather than being a mechanism of immune escape by itself [59], the additional cysteine bonds might therefore be coincidental, through the duplication of an already existing part of V1. The extra cysteines might also have facilitated the presence of the long V1 loops by stabilizing its extended structure, because if they were disadvantageous, they would probably have disappeared from the viral population. Although an extended V1 harboring additional cysteines

is not observed frequently, incorporating such V1 loops into HIV-1_{LAI} showed that HIV-1 can cope with these features via the introduction of compensatory amino acid substitutions in and around the inserted sequence (cultures 1A: L133^{dP}, M148I and T188N, and 2A: N139D and I181L; Fig. 5). Thus, while long V1 loops with additional disulfide bonds have adverse effects on Env function, sometimes leading to their deletion, they can also be accommodated by the presence of compensatory changes within the inserted segment or in close proximity of the insertion in V1 or V2. The mutations observed in culture 1A and 2A were also detected in viruses isolated from D16916 and therefore seem to facilitate the elongated V1.

Conclusions

In summary, despite the limited availability of viral samples for our study subject, our results illustrate that HIV-1 can escape from N332-directed NAb responses in a time frame of 4 months, not by changing the epitope, but by elongation of the V1 loop. The results are noteworthy in light of sequential, patient-based vaccine strategies to steer desirable Ab lineages that have the potential to become bNAbs [17, 18, 98]. Immunizing with sequential immunogens from individual D16916 will most likely not lead to development of N332-directed bNAbs when Env's with the long V1 loops are included, because in those immunogens the desired target epitope is masked. On the other hand, these same Env's more efficiently present the bNAb epitopes located at the trimer-apex. We conclude that longitudinal Env sequences should be studied in detail before using them in sequential immunization strategies.

Methods

ACS participant D16916

Individual D16916 is a male participant of the ACS who was infected in 1990 with HIV-1 subtype B, likely via IDU. He entered the ACS as HIV-1 negative and seroconverted during active follow-up, and was initially described in studies that investigated the number of ACS individuals with broad neutralization (van den Kerkhof et al. manuscript in preparation), and the longitudinal development of bNAbs in elite neutralizers ([14]; individual IDU1 in that study). D16916 was under observation for more than 12 years and until 5 years post-SC this individual had constant CD4⁺ T-cell numbers (average 395 cells/ μ l), had low/undetectable viral loads, did not receive anti-retroviral therapy and had no clinical signs of AIDS (Additional file 1: Fig. S1). In addition, this individual had no known protective human leukocyte antigen (HLA) type but was heterozygous for the Δ 32 deletion in the CCR5 gene. Serum and PBMC samples were taken approximately every 4 months. Here we studied clonal virus isolates from 7.4, 10.7, 18.8, 22.2 and 30.1 months post-SC. For

autologous neutralizing responses, we used serum samples from 7.8, 10.7, 14.1, 22.2, 34.0 and 48.9 months post-SC, whereas for heterologous neutralizing responses we used serum samples from 7.8, 10.7, 14.1, 18.8, 22.2, 26.2, 30.1, 34.0 and 37.5 months post-SC. An overview can be found in Additional file 1: Fig. S1. Rounded numbers were used in the text to refer to these time points. Due to the low viral load and limited serum availability, we were unable to extract multiple clonal virus isolates from the last three time points, as described below, or to test both autologous and heterologous neutralizing responses with sera from the same time points for all viruses.

Virus isolation from PBMCs

PBMC samples from individual D16916 were collected at month 7, 11, 19, 22 and 30 post-SC. Single clonal virus variants were isolated from selected PBMCs by direct limiting dilution of the cells. Cells were co-cultivated with PHA-stimulated PBMCs from ten healthy HIV-1 uninfected donors, as described previously [99, 100]. To prevent sequence changes during in vitro culture, the number of passages in PBMCs was kept to a minimum. An earlier study showed that the quasispecies of clonal viral variants isolated from PBMCs are highly similar to sequences from viral RNA in plasma samples from the same individual [101]. We were able to generate ten and nine replication competent clonal virus variants at 7 and 11 months post-SC, respectively, and only one viral variant at 19, 22 and 30 months post-SC, probably due to low viral loads. Furthermore, phylogenetic analyses suggested that those viruses might be archived viruses (Additional file 1: Fig. S1, Additional file 2: Fig. S2).

Gp160 sequence analysis

Proviral *env* genes from PBMCs that were infected in vitro with a single clonal HIV-1 variant were PCR-amplified and sequenced [102–104]. Nucleotide sequences were aligned using ClustalW in the software package of BioEdit [105], and edited manually, excluding contamination. The gp160 sequences were used to construct a Maximum Likelihood (ML) tree. The best-fit nucleotide substitution model (GTR + I+G), selected by hierarchical likelihood ratio tests (hLRTs, Model Test 3.7 [106]) was implemented in the heuristic search for the best ML tree applying the Tree Bisection and Reconnection (TBR) branch-swapping algorithm using PAUP*4.0 [107], starting with a neighbor-joining (NJ) tree constructed under the Hasegawa–Kishino–Yano (HKY85) model of evolution [108]. The robustness of the NJ phylogeny was assessed by bootstrap analysis with 1000 rounds of replication.

Genetic analyses were performed on gp160 sequences starting at nucleotide position 91, and for gp160 protein

analyses starting at amino acid residue 31, thereby excluding the signal peptide. PNGS, and NXT and NXS motifs were identified using *N*-glycosite [109] at the Los Alamos HIV database website (<http://www.hiv.lanl.gov/content/sequence/GLYCOSITE/glycosite.html>). Overlapping PNGS (NN[TS][ST]) were included by *N*-glycosite as one PNGS, and NPS or NPT motifs were excluded.

PBMC-based replication assays

To determine the viral replication rates of the different clonal viral variants, 2×10^6 PHA-stimulated PBMCs from ten healthy uninfected donors were inoculated with 100 50 % tissue culture infective doses (TCID₅₀) for 2 h at 37 °C in a shaking water bath, in a total volume of 2 ml. Subsequently, the PBMCs were washed with 10 ml of IMDM supplemented with 10 % fetal calf serum (FCS), and cultured in IMDM supplemented with 10 % FCS, 20 U/ml recombinant interleukin-2 (rIL-2), 5 µg/ml polybrene, 5 µg/ml ciproxine, 100 U/ml penicillin and 100 µg/ml streptomycin at a cell density of 1×10^6 per ml in a humidified CO₂-incubator at 37 °C. Experiments were performed in duplicate. At 5, 8, 11 and 14 days after inoculation, 1 ml 1×10^6 fresh PHA-stimulated PBMCs were added. Each day samples for p24 determination were taken and virus spread was analyzed with an in-house p24 antigen ELISA [110].

PBMC-based neutralization assays

For measuring neutralization, virus (30 TCID₅₀ in 25 µl when sera were tested, 20 TCID₅₀ of virus in 50 µl when bNAbs were tested) was incubated for 1 h at 37 °C with threefold serial serum dilutions starting at a dilution of 1:50, or threefold serial bNAb dilutions. The starting concentration of bNAbs was 25 µg/ml for b12 and 2G12, 10 µg/ml for 8ANC195 and 5 µg/ml for VRC01, 12A21, PG9, PG16, PGT145, PGT121. PGT126, PGT128 and PGT135. bNAbs were obtained from Herman Katinger, Peter Kwong, Michel Nussenzweig and John Mascola, directly or through the AIDS reagent program. Subsequently, 1×10^5 PHA-stimulated PBMCs were added. After an incubation of 4 h, PBMCs were washed once with 150 µl phosphate-buffered saline (PBS), put in 150 µl IMDM supplemented with 10 % FCS (inactivated at 56 °C for 30 min), 20 U/ml rIL-2, 5 µg/ml polybrene, 5 µg/ml ciproxine, 100 U/ml penicillin and 100 µg/ml streptomycin, and cultured in a humidified CO₂-incubator at 37 °C for 11 days. On days 7 and 11 virus production was measured by p24 ELISA [110]. The percent neutralization was calculated by determining the reduction in p24 production in the presence of serum or bNAbs compared to the cultures with virus only. 50 % inhibitory dose neutralization dilution (ID₅₀ values; sera) and IC₅₀ values (bNAbs) were determined by linear regression. For calculations, viruses with ID₅₀ or IC₅₀ values below the lowest

Ab concentration or above the highest Ab concentration tested were assigned the lowest or highest Ab concentration tested. For viruses that were not inhibited by the 1:50 serum dilution, we assumed that 50 % inhibition would have occurred at a 1:25 serum dilution.

Viral infection of TZM-bl cells

The TZM-bl reporter cell line stably expresses high levels of CD4-receptor and the HIV-1 coreceptors CCR5 and CXCR4 and contains the luciferase and β-galactosidase genes under control of the HIV-1 LTR promoter [111, 112]. The line was obtained through the National Institutes of Health AIDS Research and Reference Reagent Program from Dr. John C. Kappes, Dr. Xiaoyun Wu, and Tranzyme Inc., Durham, NC. TZM-bl cells were maintained in DMEM containing 10 % FCS, MEM nonessential amino acids, and penicillin/streptomycin (both at 100 U/ml). One day prior to infection, TZM-bl cells (1.7×10^4 cells) were seeded in a 96-well plate in DMEM containing 10 % FCS, MEM nonessential amino acids, and penicillin/streptomycin (both at 100 U/ml) and incubated at 37 °C in an atmosphere containing 5 % CO₂. A fixed amount of virus (500 pg) was added to the TZM-bl cells (70–80 % confluency) in the presence of 400 nM saquinavir (Roche Applied Science) and 40 µg/ml DEAE, in a total volume of 200 µl. Two days post-infection, the medium was removed, cells were washed once with PBS and subsequently lysed in Reporter Lysis buffer (Promega, Madison, WI). Luciferase activity was measured using the luciferase assay kit (Promega) and a Glomax luminometer according to the manufacturer's instructions (Turner BioSystems, Sunnyvale, CA). All infections were performed in quadruplicate. Uninfected cells were used to correct for background luciferase activity.

TZM-bl based neutralization assays

N332-glycan dependent neutralization was assessed by comparing neutralization of JRCSEF, 92BR020 and MGRM-C-026 Env-pseudotyped viruses and their N332A glycan knock-out variants with D16916 serum taken 14 months post-SC, and using BG505 Env-pseudotyped virus and its T332N knock-in variant with serum taken 30 months post-SC. Substitutions were made using the Quikchange mutagenesis kit (Agilent, Santa Clara, CA) [111]. The experiments were carried out as described previously [37]. In summary, one day prior to infection, TZM-bl cells were plated on a 96-well plate in DMEM containing 10 % FCS, $1 \times$ MEM nonessential amino acids, penicillin and streptomycin (both at 100 U/ml), and incubated at 37 °C in an atmosphere containing 5 % CO₂ for 48 h. Virus (500 pg) was incubated for 30 min at room temperature with threefold serial dilutions of serum, starting at 1:37.5 or 1:40 (after the addition of

virus). This mixture was added to the cells and 40 µg/ml DEAE, in a total volume of 200 µl. Two days later, the medium was removed. The cells were washed once with PBS (150 mM NaCl, 50 mM sodium phosphate, pH 7.0) and lysed in Reporter Lysis Buffer (Promega, Madison, WI). Luciferase activity was measured using a Luciferase Assay kit (Promega, Madison, WI) and a Glomax Luminometer according to the manufacturer's instructions (Turner BioSystems, Sunnyvale, CA). Uninfected cells were used to correct for background luciferase activity. Nonlinear regression curves were determined and IC₅₀ values were calculated using a sigmoid function in Graphpad Prism v5.01.

Construction of HIV-1_{LAI} molecular clones and generation of viruses

A slightly modified version of the full-length molecular clone HIV-1_{LAI} (pLAI; [113]) was used as the basis for introducing mutations. These modifications included the S162T, G167D, V169K and E172V substitutions, designed to restore the epitopes for bNAbs PG9 and PG16 [114]. This modified pLAI was further changed to contain V1 elongations based on the sequences observed in individual D16916 as outlined in the results section and using previously described methods [115]. Briefly, mutant *env* genes were generated in pRS1 plasmid and cloned into pLAI as Sall-BamHI fragments. Mutations, deletions, and insertions were generated using the QuikChange mutagenesis kit (Stratagene, La Jolla, CA), and the integrity of all plasmids was verified by sequencing.

Virus stocks were generated by transfecting HEK293T cells with 4 µg full-length pLAI (or mutant pLAI), using the lipofectamine method [62]. HEK293T cells were purchased from the American Type Culture Collection and cultivated in DMEM containing 10 % FCS, 1 % streptomycin and 75 mM NaHCO₃. Three days after transfection, virus-containing culture supernatants were harvested, filtered, and stored at -80 °C. Virus was quantitated by p24 ELISA [116] and viruses were normalized based on p24.

SupT1-based replication and evolution assays

SupT1 cells were maintained in DMEM supplemented with 10 % FCS, 100 U/ml penicillin and 100 µg/ml streptomycin as described previously [117], and transfected by electroporation as described previously [118]. Evolution experiments were performed essentially as described before [115, 119]. A total of 5 × 10⁶ SupT1 cells were transfected with 5 or 20 µg pLAI (or mutant pLAI), and virus spread was monitored by visual inspection for the appearance of syncytia and by p24 ELISA as indicators of virus replication. Viruses were cultured for ~3 months and decreasing amounts of supernatant were passaged

cell-free onto uninfected cells when virus replication was apparent. At regular intervals, cells and filtered supernatant were stored at -80 °C for subsequent genotypic and phenotypic analysis and virus production was quantitated by p24 ELISA. When a putative faster-replicating virus was identified, DNA was extracted from infected cells using the QIAamp DNA mini kit (Qiagen, Valencia, CA), and the complete proviral *env* sequences were PCR amplified and sequenced.

Statistical analyses

Statistical analyses were performed using Graphpad Prism v5.01. Differences between neutralizing responses were assessed using two-tailed Mann-Whitney tests, while differences in sequence (number of amino acids and PNGS) were analyzed by Student's t-tests. Correlations between gp160 sequences with p24 production per virus isolate per day and with neutralizing responses were evaluated with a linear regression model. Differences and correlations were considered statistically significant when p values were ≤0.05.

Additional files

Additional file 1: Figure S1. Longitudinal sampling, CD4⁺ T-cell count and viral RNA load during the course of infection of individual D16916. Arrows indicate the time points from which clonal HIV-1 variants were isolated (black), and from which serum was obtained for autologous and heterologous neutralization experiments (light and dark grey, respectively). CD4⁺ T-cell count (red) and HIV-1 RNA viral load measurements (black).

Additional file 2: Figure S2. Neutralization sensitivity of viral isolates for bNAbs. Clonal HIV-1 variants from 7 and 11 months post-SC were tested for their neutralization sensitivity for mAbs PGT121, PGT126, PGT128, 2G12, VRC01, PG9 and 8ANC195. The IC₅₀ values are plotted and the horizontal bars represent the median IC₅₀ value.

Additional file 3: Figure S3. Maximum-likelihood tree of longitudinal gp160 *env* sequences from isolated clonal HIV-1 variants. Clonal HIV-1 *env* sequences from 7, 11, 19, 22 and 30 months post-SC were aligned and a Maximum-likelihood (ML) tree was constructed, and are indicated in green, blue, red, purple and orange, respectively. Analyses were done with total gp160 sequences, including gaps, because for this individual the V1, harboring the additional cysteines, was of great interest.

Additional file 4: Figure S4. bNAb epitopes and the corresponding viral sequence alignment. Amino acid sequences of bNAb epitopes for isolates from 7 and 11 months post-SC. Contact residues (<5.0 Å distance from gp120 residues based on the crystal structures of gp120-bNAb co-complexes [60, 121, 122, 124] are indicated with black dots for (A) PGT135, (B) b12 (grey), 12A21 and (C) PG16.

Additional file 5: Figure S5. Schematic representation of the V1V2 loop observed in D16916. Schematic of the V1V2 loops based on Bontjer et al. [125]. Cysteine residues and disulfide bridges are indicated in red. The variable loops are depicted in yellow and the conserved bridging sheet β-strands 2 and 3, are indicated in green. (A) V1V2 loop containing the normal number of cysteine residues. (B) V1V2 loop with 2 additional cysteine and adjacent residues, forming an "oven mitt" structure. (C) V1V2 loop with 2 additional cysteine and adjacent residues, resulting in a longer V1 compared to (A). (D-E) V1V2 with 4 additional cysteine and adjacent residues forming two "oven mitt" structures, (F) or an alternative structure.

Abbreviations

HIV-1: human immunodeficiency virus type-1; bNAbs: broadly neutralizing antibodies; Env: envelope glycoprotein complex; ACS: Amsterdam Cohort Studies on HIV-1 infection and AIDS; NABs: neutralizing antibodies; C: conserved regions; V: variable regions; PNGS: potential N-linked glycosylation site(s); post-SC: post-seroconversion; WT: wild-type; CD4bs: CD4 binding site; CA: capsid; IDU: intravenous drug use; HLA: human leukocyte antigen; PHA: phytohemagglutinin; PBMCs: peripheral blood mononuclear cells; ML: maximum likelihood; hLRT: hierarchical likelihood ratio test; TBR: tree bisection and reconnection; NJ: neighbor-joining; HKY85: Hasegawa–Kishino–Yano; TCID₅₀: 50 % tissue culture infective dose; FCS: fetal calf serum; ELISA: enzyme linked immunosorbent assay; PBS: phosphate-buffered saline; rIL-2: recombinant interleukin-2; IC₅₀: 50 % inhibitory concentration; ID₅₀ dilution: 50 % inhibitory dilution.

Authors' contributions

TLGMK, SWT and BDB performed the experiments and together with RWS and MJG contributed to data acquisition. TLGMK, SWT, RWS and MJG analyzed the data. TLGMK, RWS and MJG conceived and designed the study and experiments. TLGMK, SWT, RWS and MJG wrote and TLGMK, SWT, DRB, NAK, HS, RWS and MJG edited the paper. All authors have read and approved the final manuscript.

Author details

¹ Department of Medical Microbiology, Academic Medical Center, University of Amsterdam, 1105 AZ Amsterdam, The Netherlands. ² Department of Experimental Immunology, Academic Medical Center, University of Amsterdam, 1105 AZ Amsterdam, The Netherlands. ³ Department of Immunology and Microbial Science and IAVI Neutralizing Antibody Center, The Scripps Research Institute, La Jolla, CA 92037, USA. ⁴ Ragon Institute of MGH, MIT, and Harvard, Cambridge, MA 02139, USA. ⁵ Janssen Pharmaceuticals, 2333 CN Leiden, The Netherlands. ⁶ Department of Microbiology and Immunology, Weill Medical College, Cornell University, New York, NY 10065, USA.

Acknowledgements

The Amsterdam Cohort Studies on HIV infection and AIDS, a collaboration between the Amsterdam Health Service, the Academic Medical Center of the University of Amsterdam, Sanquin Blood Supply Foundation, Medical Center Jan van Goyen and the HIV Focus Center of the DC-Clinics, are part of the Netherlands HIV Monitoring Foundation and financially supported by the Center for Infectious Disease Control of the Netherlands National Institute for Public Health and the Environment. We thank Hermann Katinger, Peter Kwong, John Mascola and Michel Nussenzweig for donating antibodies directly or through the AIDS reagents reference program.

Ethics approval and consent to participate

The Amsterdam Cohort Studies on HIV-1 infection and AIDS (ACS) are conducted in accordance with the ethical principles set out in the declaration of Helsinki, and written consent was obtained prior to data collection. The study was approved by the Academic Medical Center's Institutional Medical Ethics Committee.

Competing interests

HS is currently employed by Crucell Holland B.V., a Janssen pharmaceutical company of Johnson & Johnson, and is a Johnson & Johnson shareholder.

Funding

This study was financially supported by a Vici grant to HS from The Netherlands Organization for Scientific Research (Grant #918.66.628), a grant from the European Community's Sixth Framework Program 'European HIV Enterprise (EUOPRISE)' (FP6/2007-2012), under grant agreement 037611, and the European Community's Seventh Framework Program 'Next-Generation HIV-1 Immunogens Inducing Broadly Reactive Neutralizing Antibodies (NGIN)' (FP7/2007-2013), under grant agreement 201433. MJG receives funding from the Aids Fonds Netherlands (Grant #2012041). RWS is a recipient of a Vidi grant from the Netherlands Organization for Scientific Research (Grant #917.11.314) and a Starting Investigator Grant from the European Research Council (ERC-STG-2011-280829-SHEV). The ACS are financially supported by the Center for Infectious Disease Control of The Netherlands National Institute for Public Health and the Environment. DRB is supported by the International AIDS Vaccine Initiative through the Neutralizing Antibody Consortium and Bill

and Melinda Gates Collaboration for AIDS Vaccine Discovery and the NIAID Center for HIV/AIDS Vaccine Immunology and Immunogen Discovery Grant UM1AI100663.

Received: 16 November 2015 Accepted: 21 June 2016

Published online: 07 July 2016

References

- Doria-Rose NA, Klein RM, Manion MM, O'Dell S, Phogat A, Chakrabarti B, Hallahan CW, Migueles SA, Wrammert J, Ahmed R, et al. Frequency and phenotype of human immunodeficiency virus envelope-specific B cells from patients with broadly cross-neutralizing antibodies. *J Virol*. 2009;83:188–99.
- Euler Z, van den Kerkhof TL, van Gils MJ, Burger JA, Edo-Matas D, Phung P, Wrin T, Schuitemaker H. Longitudinal analysis of early HIV-1 specific neutralizing activity in an elite neutralizer and in five patients who developed cross-reactive neutralizing activity. *J Virol*. 2012;86:2045–55.
- Gray ES, Madiga MC, Hermanus T, Moore PL, Wibmer CK, Tumba NL, Werner L, Misana K, Sibeko S, Williamson C, et al. The neutralization breadth of HIV-1 develops incrementally over four years and is associated with CD4+ T cell decline and high viral load during acute infection. *J Virol*. 2011;85:4828–40.
- Mikell I, Sather DN, Kalams SA, Altfeld M, Alter G, Stamatatos L. Characteristics of the earliest cross-neutralizing antibody response to HIV-1. *PLoS Pathog*. 2011;7:e1001251.
- van Gils MJ, Euler Z, Schweighardt B, Wrin T, Schuitemaker H. Prevalence of cross-reactive HIV-1-neutralizing activity in HIV-1-infected patients with rapid or slow disease progression. *AIDS*. 2009;23:2405–14.
- Binley JM, Lybarger EA, Crooks ET, Seaman MS, Gray E, Davis KL, Decker JM, Wycuff D, Harris L, Hawkins G, et al. Profiling the specificity of neutralizing antibodies in a large panel of plasmas from patients chronically infected with human immunodeficiency virus type 1 subtypes B and C. *J Virol*. 2008;82:11651–68.
- Li Y, Migueles SA, Welcher B, Svehla K, Phogat A, Louder MK, Wu X, Shaw GM, Connors M, Wyatt RT, et al. Broad HIV-1 neutralization mediated by CD4-binding site antibodies. *Nat Med*. 2007;13:1032–4.
- Simek MD, Rida W, Priddy FH, Pung P, Carrow E, Laufer DS, Lehrman JK, Boaz M, Tarragona-Fiol T, Miiró G, et al. HIV-1 elite neutralizers: individuals with broad and potent neutralizing activity identified using a high throughput neutralization assay together with an analytical selection algorithm. *J Virol*. 2009;83:7337–48.
- Mascola JR, Stiegler G, VanCott TC, Katinger H, Carpenter CB, Hanson CE, Beary H, Hayes D, Frankel SS, Bix DL, et al. Protection of macaques against vaginal transmission of a pathogenic HIV-1/SIV chimeric virus by passive infusion of neutralizing antibodies. *Nat Med*. 2000;6:207–10.
- Mascola JR, Lewis MG, Stiegler G, Harris D, VanCott TC, Hayes D, Louder MK, Brown CR, Sapan CV, Frankel SS, et al. Protection of macaques against pathogenic simian/human immunodeficiency virus 89.6PD by passive transfer of neutralizing antibodies. *J Virol*. 1999;73:4009–18.
- Parren PWHI, Marx PA, Hessel AJ, Luckay A, Harouse J, Cheng-Mayer C, Moore JP, Burton DR. Antibody protects macaques against vaginal challenge with a pathogenic R5 simian/human immunodeficiency virus at serum levels giving complete neutralization in vitro. *J Virol*. 2001;75:8240–347.
- Hessel AJ, Poignard P, Hunter M, Hangartner L, Tehrani DM, Bleeker WK, Parren PW, Marx PA, Burton DR. Effective, low-titer antibody protection against low-dose repeated mucosal SHIV challenge in macaques. *Nat Med*. 2009;15:951–4.
- Hessel AJ, Rakasz EG, Poignard P, Hangartner L, Landucci G, Forthal DN, Koff WC, Watkins DI, Burton DR. Broadly neutralizing human anti-HIV antibody 2G12 is effective in protection against mucosal SHIV challenge even at low serum neutralizing titers. *PLoS Pathog*. 2009;5:e1000433.
- van den Kerkhof TL, Euler Z, van Gils MJ, Boeser-Nunnink BD, Schuitemaker H, Sanders RW. Early development of broadly reactive HIV-1 neutralizing activity in elite neutralizers. *AIDS*. 2014;28:1237–40.
- Bhiman JN, Anthony C, Doria-Rose NA, Karimanzira O, Schramm CA, Khoza T, Kitchin D, Botha G, Gorman J, Garrett NJ, et al. Viral variants that initiate and drive maturation of V1V2-directed HIV-1 broadly neutralizing antibodies. *Nat Med*. 2015;21:1332–6.

16. Gao F, Bonsignori M, Liao HX, Kumar A, Xia SM, Lu X, Cai F, Hwang KK, Song H, Zhou T, et al. Cooperation of B cell lineages in induction of HIV-1 broadly neutralizing antibodies. *Cell*. 2014;158:481–91.
17. Liao HX, Lynch R, Zhou T, Gao F, Alam SM, Boyd SD, Fire AZ, Roskin KM, Schramm CA, Zhang Z et al.: Co-evolution of a broadly neutralizing HIV-1 antibody and founder virus. *Nature*. 2013;496:469–76.
18. Doria-Rose NA, Schramm CA, Gorman J, Moore PL, Bhiman JN, DeKosky BJ, Ernandes MJ, Georgiev IS, Kim HJ, Pancera M, et al. Developmental pathway for potent V1V2-directed HIV-neutralizing antibodies. *Nature*. 2014;509:55–62.
19. Fera D, Schmidt AG, Haynes BF, Gao F, Liao HX, Kepler TB, Harrison SC. Affinity maturation in an HIV broadly neutralizing B-cell lineage through reorientation of variable domains. *Proc Natl Acad Sci USA*. 2014;111:10275–80.
20. Sather DN, Carbonetti S, Malherbe DC, Pissani F, Stuart AB, Hessel AJ, Gray MD, Mikell I, Kalams SA, Haigwood NL, et al. Emergence of broadly neutralizing antibodies and viral coevolution in two subjects during the early stages of infection with human immunodeficiency virus type 1. *J Virol*. 2014;88:12968–81.
21. Mouquet H, Scheid JF, Zoller MJ, Krogsgaard M, Ott RG, Shukair S, Artyomov MN, Pietzsch J, Connors M, Pereyra F, et al. Polyreactivity increases the apparent affinity of anti-HIV antibodies by heterologation. *Nature*. 2010;467:591–5.
22. Wu X, Yang ZY, Li Y, Hoger Corp CM, Schief WR, Seaman MS, Zhou T, Schmidt SD, Wu L, Xu L, et al. Rational design of envelope identifies broadly neutralizing human monoclonal antibodies to HIV-1. *Science*. 2010;329:856–61.
23. Scheid JF, Mouquet H, Feldhahn N, Seaman MS, Velinzon K, Pietzsch J, Ott RG, Anthony RM, Zebroski H, Hurlley A, et al. Broad diversity of neutralizing antibodies isolated from memory B cells in HIV-infected individuals. *Nature*. 2009;458:636–40.
24. Scheid JF, Mouquet H, Ueberheide B, Diskin R, Klein F, Olivera TY, Pietzsch J, Fenyo D, Abadir A, Velinzon K, et al. Sequence and structural convergence of broad and potent HIV antibodies that mimic CD4 binding. *Science*. 2011;333:1633–7.
25. Moore PL, Gray ES, Wibmer CK, Bhiman JN, Nonyane M, Sheward DJ, Hermanus T, Bajimaya S, Tumba NL, Abrahams MR et al. Evolution of an HIV glycan-dependent broadly neutralizing antibody epitope through immune escape. *Nat Med*. 2012;18:1688–92.
26. Wibmer CK, Bhiman JN, Gray ES, Tumba N, Abdool Karim SS, Williamson C, Morris L, Moore PL: Viral escape from HIV-1 neutralizing antibodies drives increased plasma neutralization breadth through sequential recognition of multiple epitopes and immunotypes. *PLoS Pathog*. 2013;9:e1003738.
27. van Gils MJ, Sanders RW. Broadly neutralizing antibodies against HIV-1: templates for a vaccine. *Virology*. 2013;435:46–56.
28. Sather DN, Armann J, Ching LK, Mavrantoni A, Sellhorn G, Caldwell Z, Yu X, Wood B, Self S, Kalams S, et al. Factors associated with the development of cross-reactive neutralizing antibodies during human immunodeficiency virus type 1 infection. *J Virol*. 2009;83:757–69.
29. Piantadosi A, Panteleeff D, Blish CA, Baeten JM, Jaoko W, McClelland RS, Overbaugh J. Breadth of neutralizing antibody response to human immunodeficiency virus type 1 is affected by factors early in infection but does not influence disease progression. *J Virol*. 2009;83:10269–74.
30. Stamatatos L, Morris L, Burton DR, Mascola JR. Neutralizing antibodies generated during natural HIV-1 infection: good news for an HIV-1 vaccine? *Nat Med*. 2009;15:866–70.
31. Bunnik EM, van Gils MJ, Lobbrecht MS, Pisas L, Nanlohy NM, Van BD, van Nuenen AC, Hessel AJ, Schuitemaker H. Emergence of b12 resistant human immunodeficiency virus type 1 variants during natural infection in the absence of humoral or cellular immune pressure. *J Gen Virol*. 2010;91:1365–72.
32. Euler Z, van Gils MJ, Bunnik EM, Phung P, Schweighardt B, Wrin T, Schuitemaker H. Cross-reactive neutralizing humoral immunity does not protect from HIV type 1 disease progression. *J Infect Dis*. 2010;201:1045–53.
33. van Gils MJ, Bunnik EM, Boeser-Nunnink BD, Burger JA, Terlouw-Klein M, Verwer N, Schuitemaker H. Longer V1V2 region with increased number of potential N-linked glycosylation sites in the HIV-1 envelope glycoprotein protects against HIV-specific neutralizing antibodies. *J Virol*. 2011;85:6986–95.
34. Walker LM, Burton DR. Rational antibody-based HIV-1 vaccine design: current approaches and future directions. *Curr Opin Immunol*. 2010;22:358–66.
35. van den Kerkhof TL, Feenstra KA, Euler Z, van Gils MJ, Rijdsdijk LW, Boeser-Nunnink BD, Heringa J, Schuitemaker H, Sanders RW. HIV-1 envelope glycoprotein signatures that correlate with the development of cross-reactive neutralizing activity. *Retrovirology*. 2013;10:102.
36. de Taeye SW, Ozorowski G, de la Torrents P, Guttman M, Julien JP, van den Kerkhof TL, Burger JA, Pritchard LK, Pugach P, Yasmeen A, et al. Immunogenicity of stabilized HIV-1 envelope trimers with reduced exposure of non-neutralizing epitopes. *Cell*. 2015;163:1702–15.
37. Sanders RW, van Gils MJ, Derking R, Sok D, Ketts TJ, Burger JA, Ozorowski G, Cupo A, Simonich C, Goo L et al. HIV-1 neutralizing antibodies induced by native-like envelope trimers. *Science*. 2015;349:6244–70.
38. Malherbe DC, Doria-Rose NA, Misher L, Beckett T, Puryear WB, Schuman JT, Kraft Z, O'Malley J, Mori M, Srivastava I, et al. Sequential immunization with a subtype B HIV-1 envelope quasiespecies partially mimics the in vivo development of neutralizing antibodies. *J Virol*. 2011;85:5262–74.
39. Pissani F, Malherbe DC, Robins H, DeFilippis VR, Park B, Sellhorn G, Stamatatos L, Overbaugh J, Haigwood NL. Motif-optimized subtype A HIV envelope-based DNA vaccines rapidly elicit neutralizing antibodies when delivered sequentially. *Vaccine*. 2012;30:5519–26.
40. Malherbe DC, Pissani F, Sather DN, Guo B, Pandey S, Sutton WF, Stuart AB, Robins H, Park B, Krebs SJ, et al. Envelope variants circulating as initial neutralization breadth developed in two HIV-infected subjects stimulate multiclade neutralizing antibodies in rabbits. *J Virol*. 2014;88:12949–67.
41. Gelderblom HR, Hausmann EHS, Ozel M, Pauli G, Koch MA. Fine structure of human immunodeficiency virus (HIV) and immunolocalization of structural proteins. *Virology*. 1987;156:171–6.
42. Julien JP, Sok D, Khayat R, Lee JH, Doores KJ, Walker LM, Ramos A, Diwanji DC, Pejchal R, Cupo A, et al. Envelope neutralizing antibody PGT121 allosterically modulates CD4 binding via recognition of the HIV-1 gp120 V3 base and multiple surrounding glycans. *PLoS Pathog*. 2013;9:e1003342.
43. Pancera M, Zhou T, Druz A, Georgiev IS, Soto C, Gorman J, Huang J, Acharya P, Chuang GY, Ofek G, et al. Structure and immune recognition of trimeric pre-fusion HIV-1 Env. *Nature*. 2014;514:455–61.
44. Checkley MA, Lutttge BG, Freed EO. HIV-1 envelope glycoprotein biosynthesis, trafficking, and incorporation. *J Mol Biol*. 2011;410:582–608.
45. Willey RL, Rutledge RA, Dias S, Folks T, Theodore T, Buckler CE, Martin MA. Identification of conserved and divergent domains within the envelope gene of the acquired immunodeficiency syndrome retrovirus. *Proc Natl Acad Sci USA*. 1986;83:5038–42.
46. Starcich BR, Hahn BH, Shaw GM, McNeely PD, Modrow S, Wolf H, Parks ES, Parks WP, Josephs SF, Gallo RC, et al. Identification and characterization of conserved and variable regions in the envelope gene of HTLV-III/LAV, the retrovirus of AIDS. *Cell*. 1986;45:637–48.
47. Allan JS, Coligan JE, Bariun F, et al. Major glycoprotein antigens that induce antibodies in AIDS patients are encoded by HTLV-III. *Science*. 1985;228:1091–3.
48. Binley JM, Ban YE, Crooks ET, Eggink D, Osawa K, Schief WR, Sanders RW. Role of complex carbohydrates in human immunodeficiency virus type 1 infection and resistance to antibody neutralization. *J Virol*. 2010;84:5637–55.
49. Reitter JN, Means RE, Desrosiers RC. A role for carbohydrates in immune evasion in AIDS. *Nat Med*. 1998;4:679–84.
50. Aasa-Chapman MM, Hayman A, Newton P, Cornforth D, Williams I, Borrow P, Balfe P, McKnight A. Development of the antibody response in acute HIV-1 infection. *AIDS*. 2004;18:371–81.
51. Wei X, Decker JM, Wang S, Hui H, Kappes JC, Wu X, Salazar-Gonzalez JF, Salazar MG, Kilby JM, Saag MS, et al. Antibody neutralization and escape by HIV-1. *Nature*. 2003;422:307–12.
52. Richman DD, Little SJ, Smith DM, Wrin T, Petropoulos C, Wong JK. HIV evolution and escape. *Trans Am Clin Climatol Assoc*. 2004;115:289–303.
53. Leonard CK, Spellman MW, Riddle L, Harris RJ, Thomas JN, Gregory TJ. Assignment of interchain disulfide bonds and characterization of potential glycosylation sites of the type 1 recombinant human immunodeficiency virus envelope glycoprotein (gp120) expressed in chinese hamster ovary cells. *J Biol Chem*. 1990;265:10373–82.

54. van Anken E, Sanders RW, Liscaljet IM, Land A, Bontjer I, Tillemans S, Nabatov AA, Paxton WA, Berkhout B, Braakman L. Only five of 10 strictly conserved disulfide bonds are essential for folding and eight for function of the HIV-1 envelope glycoprotein. *Mol Biol Cell*. 2008;19:4298–309.
55. McCutchan FE, Hegerich PA, Brennan TP. Genetic variants of HIV-1 in Thailand. *AIDS Res Hum Retroviruses*. 1992;8:1887–95.
56. McCutchan FE, Arstenstein AW, Sanders-Buell E, Salminen MO, Carr JK, Mascola JR, Yu XF, Nelson KE, Khamboonruang C, Schmitt D, et al. Diversity of the envelope glycoprotein among human immunodeficiency virus type 1 isolates of clade E from Asia and Africa. *J Virol*. 1996;70:3331–8.
57. Wang WK, Mayer KH, Essex M, Lee TH. Sequential change of cysteine residues in hypervariable region 1 of glycoprotein 120 in primary HIV type 1 isolates of subtype B. *AIDS Res Hum Retroviruses*. 1996;12:1195–7.
58. Wang WK, Essex M, Lee TH. Uncommon gp120 cysteine residues found in primary HIV-1 isolates. *AIDS Res Hum Retroviruses*. 1995;11:185–8.
59. Jobes DV, Daoust M, Nguyen V, Padua A, Michele S, Lock MD, Chen A, Sinangil F, Berman PW. High incidence of unusual cysteine variants in gp120 envelope proteins from early HIV type 1 infections from a Phase 3 vaccine efficacy trial. *AIDS Res Hum Retroviruses*. 2006;22:1014–21.
60. Kong L, Lee JH, Doores KJ, Murin CD, Julien JP, McBride R, Liu Y, Marozsan A, Cupo A, Klasse PJ et al. Supersite of immune vulnerability on the glycosylated face of HIV-1 envelope glycoprotein gp120. *Nat Struct Mol Biol*. 2013;20:796–803.
61. Walker LM, Huber M, Doores KJ, Falkowska E, Pejchal R, Julien JP, Wang SK, Ramos A, Chan-Hui PY, Moyle M, et al. Broad neutralization coverage of HIV by multiple highly potent antibodies. *Nature*. 2011;477:466–70.
62. Sanders RW, Derking R, Cupo A, Julien JP, Yasmeen A, de Val N, Kim HJ, Blattner C, de la Pena AT, Korzun J, et al. A next-generation cleaved, soluble HIV-1 Env trimer, BG505 SOSIP.664 gp140, expresses multiple epitopes for broadly neutralizing but not non-neutralizing antibodies. *PLoS Pathog*. 2013;9:e1003618.
63. Gavel Y, von Heijne G. Sequence differences between glycosylated and non-glycosylated Asn-X-Thr/Ser acceptor sites: implications for protein engineering. *Protein Eng*. 1990;3:433–42.
64. Kaplan HA, Welply JK, Lennarz WJ. Oligosaccharyl transferase: the central enzyme in the pathway of glycoprotein assembly. *Biochim Biophys Acta*. 1987;906:161–73.
65. Shakin-Eshleman SH, Spitalnik SL, Kasturi L. The amino acid at the X position of an Asn-X-Ser sequon is an important determinant of N-linked core-glycosylation efficiency. *J Biol Chem*. 1996;271:6363–6.
66. Richman DD, Wrin T, Little SJ, Petropoulos CJ. Rapid evolution of the neutralizing antibody response to HIV type 1 infection. *Proc Natl Acad Sci USA*. 2003;100:4144–9.
67. Moore PL, Ranchobe N, Lambson BE, Gray ES, Cave E, Abrahams MR, Bandawe G, Mlisana K, Bdool Karim SS, Williamson C, et al. Limited neutralizing antibody specificities drive neutralization escape in early HIV-1 subtype C infection. *PLoS Pathog*. 2009;5:e1000598.
68. Moore PL, Williamson C, Morris L. Virological features associated with the development of broadly neutralizing antibodies to HIV-1. *Trends Microbiol*. 2015;23:204–11.
69. Sok D, Doores KJ, Briney B, Le KM, Saye-Francisco KL, Ramos A, Kulp DW, Julien JP, Menis S, Wickramasinghe L, et al. Promiscuous glycan site recognition by antibodies to the high-mannose patch of gp120 broadens neutralization of HIV. *Sci Transl Med*. 2014;6:236ra63.
70. Garces F, Sok D, Kong L, McBride R, Kim HJ, Saye-Francisco KF, Julien JP, Hua Y, Cupo A, Moore JP, et al. Structural evolution of glycan recognition by a family of potent HIV antibodies. *Cell*. 2014;159:69–79.
71. Murphy MK, Yue L, Pan R, Boliar S, Sethi A, Tian J, Pfafferot K, Karita E, Allen SA, Cormier E, et al. Viral escape from neutralizing antibodies in early subtype A HIV-1 infection drives an increase in autologous neutralization breadth. *PLoS Pathog*. 2013;9:e1003173.
72. Sadjadpour R, Donau OK, Shingai M, Buckler-White A, Kao S, Strebel K, Nishimura Y, Martin MA. Emergence of gp120 V3 variants confers neutralization resistance in an R5 simian-human immunodeficiency virus-infected macaque elite neutralizer that targets the N332 glycan of the human immunodeficiency virus type 1 envelope glycoprotein. *J Virol*. 2013;87:8798–804.
73. Shingai M, Nishimura Y, Klein F, Mouquet H, Donau OK, Plishka R, Buckler-White A, Seaman M, Piatak M Jr, Lifson JD, et al. Antibody-mediated immunotherapy of macaques chronically infected with SHIV suppresses viraemia. *Nature*. 2013;503:277–80.
74. Klein F, Halper-Stromberg A, Horwitz JA, Gruell H, Scheid JF, Bournazos S, Mouquet H, Spatz LA, Diskin R, Abadir A, et al. HIV therapy by a combination of broadly neutralizing antibodies in humanized mice. *Nature*. 2012;492:118–22.
75. Horwitz JA, Halper-Stromberg A, Mouquet H, Gitlin AD, Tretiakova A, Eisenreich TR, Malbec M, Gravemann S, Billerbeck E, Dorner M, et al. HIV-1 suppression and durable control by combining single broadly neutralizing antibodies and antiretroviral drugs in humanized mice. *Proc Natl Acad Sci USA*. 2013;110:16538–43.
76. Nishimura Y, Shingai M, Willey R, Sadjadpour R, Lee WR, Brown CR, Brechley JM, Buckler-White A, Petros R, Eckhaus M, et al. Generation of the pathogenic R5-tropic simian/human immunodeficiency virus SH1-VAD8 by serial passaging in rhesus macaques. *J Virol*. 2010;84:4769–81.
77. Walker LM, Sok D, Nishimura Y, Donau O, Sadjadpour R, Gautam R, Shingai M, Pejchal R, Ramos A, Simek MD, et al. Rapid development of glycan-specific, broad, and potent anti-HIV-1 gp120 neutralizing antibodies in an R5 SHIV/HIV chimeric virus infected macaque. *Proc Natl Acad Sci USA*. 2011;108:20125–9.
78. Rong R, Li B, Lynch RM, Haaland RE, Murphy MK, Mulenga J, Allen SA, Pinter A, Shaw GM, Hunter E, et al. Escape from autologous neutralizing antibodies in acute/early subtype C HIV-1 infection requires multiple pathways. *PLoS Pathog*. 2009;5:e1000594.
79. Zolla-Pazner S. Identifying epitopes of HIV-1 that induce protective antibodies. *Nat Rev Immunol*. 2004;4:199–210.
80. Stamatatos L, Cheng-Mayer C. An envelope modification that renders a primary, neutralization-resistant clade B human immunodeficiency virus type 1 isolate highly susceptible to neutralization by sera from other clades. *J Virol*. 1998;72:7840–5.
81. O'Rourke SM, Schweighardt B, Phung P, Fonseca DP, Terry K, Wrin T, Sinangil F, Berman PW. Mutation at a single position in the V2 domain of the HIV-1 envelope protein confers neutralization sensitivity to a highly neutralization-resistant virus. *J Virol*. 2010;84:11200–9.
82. Ly A, Stamatatos L. V2 loop glycosylation of the human immunodeficiency virus type 1 SF162 envelope facilitates interaction of this protein with CD4 and CCR5 receptors and protects the virus from neutralization by anti-V3 loop and anti-CD4 binding site antibodies. *J Virol*. 2000;74:6769–76.
83. Pinter A, Honnen WJ, He Y, Gorny MK, Zolla-Pazner S, Kayman SC. The V1/V2 domain of gp120 is a global regulator of the sensitivity of primary human immunodeficiency virus type 1 isolates to neutralization by antibodies commonly induced upon infection. *J Virol*. 2004;78:5205–15.
84. Sagar M, Wu X, Lee S, Overbaugh J. Human immunodeficiency virus type 1 V1–V2 envelope loop sequences expand and add glycosylation sites over the course of infection, and these modifications affect antibody neutralization sensitivity. *J Virol*. 2006;80:9586–98.
85. Li Y, Cleveland B, Klots I, Travis B, Richardson BA, Anderson D, Montefiori D, Polacino P, Hu SL. Removal of a single N-linked glycan in human immunodeficiency virus type 1 gp120 results in an enhanced ability to induce neutralizing antibody responses. *J Virol*. 2008;82:638–51.
86. Ye Y, Si ZH, Moore JP, Sodroski J. Association of structural changes in the V2 and V3 loops of the gp120 envelope glycoprotein with acquisition of neutralization resistance in a simian-human immunodeficiency virus passaged in vivo. *J Virol*. 2000;74:11955–62.
87. Guttman M, Kahn M, Garcia NK, Hu SL, Lee KK. Solution structure, conformational dynamics, and CD4-induced activation in full-length, glycosylated, monomeric HIV gp120. *J Virol*. 2012;86:8750–64.
88. Watkins JD, Diaz-Rodriguez J, Siddappa NB, Corti D, Ruprecht RM. Efficiency of neutralizing antibodies targeting the CD4-binding site: influence of conformational masking by the V2 loop in R5-tropic clade C simian-human immunodeficiency virus. *J Virol*. 2011;85:12811–4.
89. Liu L, Cimbro R, Lusso P, Berger EA. Intraprotomer masking of third variable loop (V3) epitopes by the first and second variable loops (V1V2) within the native HIV-1 envelope glycoprotein trimer. *Proc Natl Acad Sci USA*. 2011;108:20148–53.

90. Rusert P, Krarup A, Magnus C, Brandenberg OF, Weber J, Ehler AK, Regoes RR, Gunthard HF, Trkola A. Interaction of the gp120 V1V2 loop with a neighboring gp120 unit shields the HIV envelope trimer against cross-neutralizing antibodies. *J Exp Med*. 2011;208:1419–33.
91. Julien JP, Cupo A, Sok D, Stanfield RL, Lyumkis D, Deller MC, Klasse PJ, Burton DR, Sanders RW, Moore JP, et al. Crystal structure of a soluble cleaved HIV-1 envelope trimer. *Science*. 2013;342:1477–83.
92. Lyumkis D, Julien JP, de Val N, Cupo A, Potter CS, Klasse PJ, Burton DR, Sanders RW, Moore JP, Carragher B, et al. Cryo-EM structure of a fully glycosylated soluble cleaved HIV-1 envelope trimer. *Science*. 2013;342:1484–90.
93. Bar KJ, Tsao CY, Iyer SS, Decker JM, Yang Y, Bonsignori M, Chen X, Hwang KK, Montefiori DC, Liao HX, et al. Early low-titer neutralizing antibodies impede HIV-1 replication and select for virus escape. *PLoS Pathog*. 2012;8:e1002721.
94. Quakkelaar ED, Bunnik EM, van Alphen FP, Boeser-Nunnink BD, van Nuenen AC, Schuitemaker H. Escape of human immunodeficiency virus type 1 from broadly neutralizing antibodies is not associated with a reduction of viral replicative capacity in vitro. *Virology*. 2007;363:447–53.
95. van Gils MJ, Bunnik EM, Burger JA, Jacob Y, Schweighardt B, Wrin T, Schuitemaker H. Rapid escape from preserved cross-reactive neutralizing humoral immunity without loss of viral fitness in HIV-1-infected progressors and long-term nonprogressors. *J Virol*. 2010;84:3576–85.
96. Sather DN, Carbonetti S, Kehayia J, Kraft Z, Mikell I, Scheid JF, Klein F, Stamatatos L. Broadly neutralizing antibodies developed by an HIV-positive elite neutralizer exact a replication fitness cost on the contemporaneous virus. *J Virol*. 2012;86:12676–85.
97. Bunnik EM, Lobbrecht MS, van Nuenen AC, Schuitemaker H. Escape from autologous humoral immunity of HIV-1 is not associated with a decrease in replicative capacity. *Virology*. 2010;397:224–30.
98. Haynes BF, Kelsoe G, Harrison SC, Kepler TB. B-cell-lineage immunogen design in vaccine development with HIV-1 as a case study. *Nat Biotechnol*. 2012;30:423–33.
99. Van't Wout AB, Schuitemaker H, Kootstra NA. Isolation and propagation of HIV-1 on peripheral blood mononuclear cells. *Nat Protoc*. 2008;3:363–70.
100. Schuitemaker H, Koot M, Kootstra NA, Dercksen MW, De Goede REY, Van Steenwijk RP, Lange JMA, Eeftink Schattenkerk JKM, Miedema F, Tersmette M. Biological phenotype of human immunodeficiency virus type 1 clones at different stages of infection: progression of disease is associated with a shift from monocytotropic to T-cell-tropic virus populations. *J Virol*. 1992;66:1354–60.
101. Edo-Matas D, van Gils MJ, Bowles EJ, Navis M, Rächinger A, Boeser-Nunnink B, Stewart-Jones GB, Kootstra NA, Wout AB, Schuitemaker H. Genetic composition of replication competent clonal HIV-1 variants isolated from peripheral blood mononuclear cells (PBMC), HIV-1 proviral DNA from PBMC and HIV-1 RNA in serum in the course of HIV-1 infection. *Virology*. 2010;405:492–504.
102. Beaumont T, van Nuenen A, Broersen S, Blattner WA, Lukashov VV, Schuitemaker H. Reversal of HIV-1 IIIB towards a neutralization resistant phenotype in an accidentally infected laboratory worker with a progressive clinical course. *J Virol*. 2001;75:2246–52.
103. Boom R, Sol CJA, Salimans MMM, Jansen CL, Wertheim-van Dillen PME, Van der Noordaa J. A rapid and simple method for purification of nucleic acids. *J Clin Microbiol*. 1991;28:495–503.
104. Quakkelaar ED, van Alphen FP, Boeser-Nunnink BD, van Nuenen AC, Pantophlet R, Schuitemaker H. Susceptibility of recently transmitted subtype B human immunodeficiency virus type 1 variants to broadly neutralizing antibodies. *J Virol*. 2007;81:8533–42.
105. Hall TA. BioEdit: a user-friendly biological sequence alignment editor and analysis program for Windows 95/98/NT. *Nucl Acids Symp Ser*. 1999;41:95–8.
106. Posada D, Crandall KA. Modeltest: testing the model of DNA substitution. *Bioinformatics*. 1998;14:817–8.
107. Wilgenbusch JC, Swofford D. Inferring evolutionary trees with PAUP. *Curr Protoc Bioinformatics*. 2003;Chapter 6:Unit 6.4. doi:10.1002/0471250953.bi0604s00
108. Hasegawa M, Kishino H, Yano T. Dating of the human-ape splitting by a molecular clock of mitochondrial DNA. *J Mol Evol*. 1985;22:160–74.
109. Zhang M, Gaschen B, Blay W, Foley B, Haigwood N, Kuiken C, Korber B. Tracking global patterns of N-linked glycosylation site variation in highly variable viral glycoproteins: HIV, SIV, and HCV envelopes and influenza hemagglutinin. *Glycobiology*. 2004;14:1229–46.
110. Tersmette M, Winkel IN, Groenink M, Gruters RA, Spence P, Saman E, van der Groen G, Miedema F, Huisman JG. Detection and subtyping of HIV-1 isolates with a panel of characterized monoclonal antibodies to HIV-p24 gag. *Virology*. 1989;171:149–55.
111. Wei X, Decker JM, Liu H, Zhang Z, Arani RB, Kilby JM, Saag MS, Wu X, Shaw GM, Kappes JC. Emergence of resistant human immunodeficiency virus type 1 in patients receiving fusion inhibitor (T-20) monotherapy. *Antimicrob Agents Chemother*. 2002;46:1896–905.
112. Walker LM, Phogat SK, Chan-Hui PY, Wagner D, Phung P, Goss JL, Wrin T, Simek MD, Flinn S, Mitcham JL, et al. Broad and Potent Neutralizing Antibodies from an African Donor Reveal a New HIV-1 Vaccine Target. *Science*. 2009;326:285–9.
113. Peden K, Emerman M, Montagnier L. Changes in growth properties on passage in tissue culture of viruses derived from infectious molecular clones of HIV-1LAI, HIV-1MAL, and HIV-1ELI. *Virology*. 1991;185:661–72.
114. Ringe R, Phogat S, Bhattacharya J. Subtle alteration of residues including N-linked glycans in V2 loop modulate HIV-1 neutralization by PG9 and PG16 monoclonal antibodies. *Virology*. 2012;426:34–41.
115. Sanders RW, Dankers MM, Busser E, Caffrey M, Moore JP, Berkhout B. Evolution of the HIV-1 envelope glycoproteins with a disulfide bond between gp120 and gp41. *Retrovirology*. 2004;1:3.
116. Jeeninga RE, Hoogenkamp M, Armand-Ugon M, de Baar M, Verhoef K, Berkhout B. Functional differences between the long terminal repeat transcriptional promoters of human immunodeficiency virus type 1 subtypes A through G. *J Virol*. 2000;74:3740–51.
117. Sanders RW, de Jong EC, Baldwin CE, Schuitemaker JH, Kapsenberg ML, Berkhout B. Differential transmission of human immunodeficiency virus type 1 by distinct subsets of effector dendritic cells. *J Virol*. 2002;76:7812–21.
118. Das AT, Land A, Braakman I, Klaver B, Berkhout B. HIV-1 evolves into a nonsyncytium-inducing virus upon prolonged culture in vitro. *Virology*. 1999;263:55–69.
119. Sanders RW, Busser E, Moore JP, Lu M, Berkhout B. Evolutionary repair of HIV type 1 gp41 with a kink in the N-terminal helix leads to restoration of the six-helix bundle structure. *AIDS Res Hum Retroviruses*. 2004;20:742–9.
120. Garces F, Lee JH, de Val N, de la Torrents P, Kong L, Puchades C, Hua Y, Stanfield RL, Burton DR, Moore JP, et al. Affinity maturation of a potent family of HIV antibodies is primarily focused on accommodating or avoiding glycans. *Immunity*. 2015;43:1053–63.
121. Zhou T, Xu L, Dey B, Hessell AJ, Van RD, Xiang SH, Yang X, Zhang MY, Zwick MB, Arthos J, et al. Structural definition of a conserved neutralization epitope on HIV-1 gp120. *Nature*. 2007;445:732–7.
122. Klein F, Diskin R, Scheid JF, Gaebler C, Mouquet H, Georgiev IS, Pancera M, Zhou T, Incesu RB, Fu BZ, et al. Somatic mutations of the immunoglobulin framework are generally required for broad and potent HIV-1 neutralization. *Cell*. 2013;153:126–38.
123. Zhou T, Georgiev I, Wu X, Yang ZY, Dai K, Finzi A, Do KY, Scheid J, Shi W, Xu L, et al. Structural basis for broad and potent neutralization of HIV-1 by antibody VRC01. *Science*. 2010;329:811–7.
124. Pancera M, Shahzad-ul-Hussan S, Doria-Rose NA, McLellan JS, Bailer RT, Dai K, Loesgen S, Louder MK, Staube RP, Yang Y, et al. Structural basis for diverse N-glycan recognition by HIV-1-neutralizing V1–V2-directed antibody PG16. *Nat Struct Mol Biol*. 2013;20:804–13.
125. Bontjer I, Land A, Eggink D, Verkade E, Tuin K, Baldwin C, Pollakis G, Paxton WA, Braakman I, Berkhout B, et al. Optimization of human immunodeficiency virus type 1 envelope glycoproteins with V1/V2 deleted, using virus evolution. *J Virol*. 2009;83:368–83.